Progress In Electromagnetics Research, Vol. 134, 475–507, 2013

FINITE DATA PERFORMANCE ANALYSIS OF MVDR ANTENNA ARRAY BEAMFORMERS WITH DIAGONAL LOADING

Yen-Lin Chen[1] and Ju-Hong Lee[2, 3, *]

[1]Graduate Institute of Communication Engineering, National Taiwan University, No. 1, Section 4, Roosevelt Road, Taipei 10617, Taiwan

[2]Department of Electrical Engineering, Graduate Institute of Communication Engineering, National Taiwan University, No. 1, Section 4, Roosevelt Road, Taipei 10617, Taiwan

[3]Graduate Institute of Biomedical Electronics and Bioinformatics, National Taiwan University, No. 1, Section 4, Roosevelt Road, Taipei 10617, Taiwan

Abstract—Diagonal loading has been regarded as an efficient manner to tackle the finite sample effect or the steering vector imprecision problem on adaptive array beamforming. However, the reason of the robustness improvement by the loading factor is still unknown and rarely discussed. In this paper, we consider the finite sample effect and derive the approximated output signal-to-interference-plus-noise ratio (SINR) of minimum variance distortionless response (MVDR) beamformers with diagonal loading. The obtained SINR expression is more explicit and compact than the existing formulas in the literature. Based on the theoretical results, we investigate the effects of a loading factor on the output SINR of MVDR beamformers. The theoretical analysis shows the effectiveness of diagonal loading on alleviating finite sample effect. Moreover, the price of using diagonal loading is also discussed. Simulation results are presented for confirming the validity of the research work.

1. INTRODUCTION

Adaptive arrays have been utilized in a variety of fields due to the anti-interference abilities and superior resolutions. Among the techniques

Received 20 September 2012, Accepted 21 November 2012, Scheduled 6 December 2012

* Corresponding author: Ju-Hong Lee (juhong@cc.ee.ntu.edu.tw).

for adaptive array beamforming, the minimum variance distortionless response (MVDR) technique [1] is the most popular one used for finding the required adaptive weights. When the second-order statistics of the received array data vector and the steering vector of the desired signal are exactly known, a MVDR beamformer can eliminate the interferers and noise efficiently without imposing distortion in the reception of the desired signal. However, the performance of a MVDR beamformer could be deteriorated by several unavoidable errors in practical situations, such as finite sample effect [2–12], mutual coupling effect [13, 14], steering vector uncertainty [15–19], etc.. To alleviate the effects due to the errors on adaptive arrays, many robust methods for improving array performance were proposed and analyzed during the past decades. Notable among them are the eigenspace-based methods [19, 20], spatial smoothing technique [21], signal blocking based beamformer [22], and diagonal loading techniques [23–27].

A diagonal loading technique is carried out by adding a real value called loading factor on the diagonal entries of the correlation matrix of the received array data vector. It has been shown that the diagonal loading techniques are effective in dealing with steering vector errors and finite sample effect if an appropriate loading factor is used. Research endeavor has been devoted to finding an optimum loading factor [28–30]. However, it is also critical to evaluate the effects of a loading factor on the performance of a MVDR beamformer. Several reports regarding the performance of MVDR beamformers with diagonal loading under finite samples can be found in [8–11]. Fertig [8] derived the probability density function of the beam response of MVDR beamformers with diagonal loading. Liu et al. [9] gave a short discussion on the impact of diagonal loading on the detection probability and output waveform for space-time adaptive processing. Dilsavor and Moses [10] analyzed the mean and variance of the weight, the output power, the output SINR, and the interference-to-noise ratio. The formulas in [10] are derived by approximating the higher order terms of the power series. However, the effects of positive loading factors were rarely discussed. Recently, Mestre and Lagunas [11] presented an output signal-to-interference-plus-noise ratio (SINR) formula for the MVDR beamformer with diagonal loading and proposed a feasible method to compute the optimum loading factor. Based on the random matrix theory, this formula is obtained under the assumptions of both the number m of snapshots and the number p of array elements increasing without bound and the ratio m/p fixed at a constant. Although the formula proposed in [11] can be used under finite sample effect and steering vector errors, it is difficult to realize how the loading factor mitigates the performance

degradation according to the complicated expression. Besides, the analytical result in [11] sometimes fails to predict the actual output SINR well, especially when the desired signal is strong.

In this paper, we derive approximated expressions for the output SINR of MVDR beamformers with diagonal loading. Utilizing the approximation for the weight vector presented by Wax and Anu [5], a general output SINR formula in terms of interference-plus-noise correlation matrix is first derived. Then, we narrow the scope to one desired signal and two interferers and obtain a more explicit output SINR expression in terms of system parameters. Based on this explicit result, the effects of the loading factor on the output SINR under finite samples are discussed in detail. The pros and cons of using diagonal loading are shown clearly. Moreover, the possibility of generalizing the explicit formula to the multi-interference case is explored. The validity of the theoretical work is confirmed by simulation results.

The remaining part of this paper is organized as follows. The principles of MVDR beamformers with diagonal loading and the definition of output SINR are described in Section 2. The output SINR of MVDR beamformers with diagonal loading is derived in Section 3. Discussions on the theoretical results are presented in Section 4. Simulations are performed in Section 5 to confirm the theoretical results. Finally, we make a conclusion in Section 6.

2. PROBLEM FORMULATION

2.1. Principles of MVDR Beamformers

Consider a p-element array beamformer impinged by q narrowband signals including one desired signal and $(q-1)$ interferers, $q < p$. The received data vector can be expressed as

$$\mathbf{x}(t) = s_1(t)\,\mathbf{a}_1 + \sum_{r=2}^{q} s_r(t)\,\mathbf{a}_r + \mathbf{n}(t) = s_1(t)\,\mathbf{a}_1 + \mathbf{v}(t), \qquad (1)$$

where $s_i(t)$ is the complex waveform of the ith signal source with zero mean and variance σ_{si}^2, $\mathbf{a}_i$ the corresponding steering vector, $\mathbf{n}(t)$ the additive white Gaussian noise vector with zero mean and variance σ_n^2, and $\mathbf{v}(t)$ the undesired component including the interference and noise. Assume that the q signal sources and noise are mutually independent. The ensemble correlation matrices of $\mathbf{x}(t)$ and $\mathbf{v}(t)$ are respectively given by

$$\mathbf{R} \equiv E\left[\mathbf{x}(t)\,\mathbf{x}^H(t)\right] = \sigma_{s1}^2\mathbf{a}_1\mathbf{a}_1^H + \mathbf{Q} \qquad (2)$$

$$\text{and} \quad \mathbf{Q} \equiv E\left[\mathbf{v}\left(t\right)\mathbf{v}^{H}\left(t\right)\right] = \sum_{r=2}^{q} \sigma_{sr}^{2}\mathbf{a}_{r}\mathbf{a}_{r}^{H} + \sigma_{n}^{2}\mathbf{I}, \tag{3}$$

where $E[\cdot]$ is the mathematical expectation, $\{\cdot\}^{H}$ denotes the conjugate and transpose operation, and $\mathbf{I}$ is the identity matrix with appropriate size. The weight vector of a MVDR beamformer can be found by solving the following optimization problem [1]:

$$\text{Minimize } \mathbf{w}^{H}\mathbf{R}\mathbf{w} \quad \text{Subject to} \quad \mathbf{w}^{H}\mathbf{a}_{1} = 1. \tag{4}$$

From (4), we have the optimal weight vector $\mathbf{w}_o$ given by [1]

$$\mathbf{w}_{o} = \frac{\mathbf{R}^{-1}\mathbf{a}_{1}}{\mathbf{a}_{1}^{H}\mathbf{R}^{-1}\mathbf{a}_{1}}, \tag{5}$$

where $\{\cdot\}^{-1}$ denotes the inverse of a matrix. Using (2) and applying the matrix inversion lemma, the optimal weight vector in (5) can also be written as

$$\mathbf{w}_{o} = \frac{\mathbf{Q}^{-1}\mathbf{a}_{1}}{\mathbf{a}_{1}^{H}\mathbf{Q}^{-1}\mathbf{a}_{1}}. \tag{6}$$

In practice, only finite data samples are available. The ensemble matrix $\mathbf{R}$ is approximated by a sample correlation matrix using m data samples as follows:

$$\hat{\mathbf{R}} = \frac{1}{m}\sum_{i=1}^{m} \mathbf{x}\left(t_{i}\right)\mathbf{x}^{H}\left(t_{i}\right), \tag{7}$$

where $\mathbf{x}(t_i)$ denotes the data vector $\mathbf{x}(t)$ taken at the time instant t_i. The weight vector in (5) becomes

$$\hat{\mathbf{w}} = \frac{\hat{\mathbf{R}}^{-1}\mathbf{a}_{1}}{\mathbf{a}_{1}^{H}\hat{\mathbf{R}}^{-1}\mathbf{a}_{1}}. \tag{8}$$

Although the weight vector $\hat{\mathbf{w}}$ satisfies the unit-gain constraint in (4), it does not minimize the array output power due to the use of finite data samples. The diagonal loading technique adding a loading factor κ to all diagonal entries of $\hat{\mathbf{R}}$ could provide robustness against the finite sample effect [6]. The weight vector of a MVDR beamformer with diagonal loading is given by [25, 29]

$$\hat{\mathbf{w}}_{D} = \frac{\left(\hat{\mathbf{R}} + \kappa \cdot \mathbf{I}\right)^{-1}\mathbf{a}_{1}}{\mathbf{a}_{1}^{H}\left(\hat{\mathbf{R}} + \kappa \cdot \mathbf{I}\right)^{-1}\mathbf{a}_{1}} = \frac{\hat{\mathbf{R}}_{D}^{-1}\mathbf{a}_{1}}{\mathbf{a}_{1}^{H}\hat{\mathbf{R}}_{D}^{-1}\mathbf{a}_{1}}, \tag{9}$$

where the subscript D denotes the MVDR beamformer with diagonal loading and $\hat{\mathbf{R}}_{D} \equiv \hat{\mathbf{R}} + \kappa \cdot \mathbf{I}$ is the diagonal-loaded correlation matrix.

The $\hat{\mathbf{w}}_D$ of (9) still holds the unit-gain constraint in (4). However, its output power is different from that produced by $\hat{\mathbf{w}}$. Substituting (1) into (7), we have $\hat{\mathbf{R}}$ and $\hat{\mathbf{R}}_D$ given by

$$\hat{\mathbf{R}} = \hat{\sigma}_{s1}^2 \mathbf{a}_1 \mathbf{a}_1^H + \mathbf{a}_1 \hat{\mathbf{r}}^H + \hat{\mathbf{r}} \mathbf{a}_1^H + \hat{\mathbf{Q}} \tag{10}$$

$$\text{and} \quad \hat{\mathbf{R}}_D = \hat{\sigma}_{s1}^2 \mathbf{a}_1 \mathbf{a}_1^H + \mathbf{a}_1 \hat{\mathbf{r}}^H + \hat{\mathbf{r}} \mathbf{a}_1^H + \hat{\mathbf{Q}}_D, \tag{11}$$

where $\hat{\sigma}_{s1}^2 = (1/m) \sum_{i=1}^m |s_1(t_i)|^2$, $\hat{\mathbf{r}} = (1/m) \sum_{i=1}^m s_1^*(t_i) \mathbf{v}(t_i)$, $\hat{\mathbf{Q}} = (1/m) \sum_{i=1}^m \mathbf{v}(t_i) \mathbf{v}^H(t_i)$, and $\hat{\mathbf{Q}}_D \equiv \hat{\mathbf{Q}} + \kappa \cdot \mathbf{I}$. Using the assumptions of independence and zero mean for the signal sources and noise, two statistical properties of $\hat{\mathbf{r}}$ are given as follows [5, 12]:

$$E[\hat{\mathbf{r}}] = \mathbf{0} \tag{12}$$

$$\text{and} \quad E\left[\hat{\mathbf{r}} \hat{\mathbf{r}}^H\right] = \frac{\sigma_{s1}^2}{m} \mathbf{Q}. \tag{13}$$

2.2. The Output SINR and the Existing Analysis Results

The SINR of an array output is one of the most popular quantities to evaluate the performance of adaptive beamforming. Let the weight vector of an array beamformer be denoted by $\mathbf{w}$. The output signal and the corresponding output power are given by

$$y(t) = \mathbf{w}^H \mathbf{x}(t) \tag{14}$$

$$\begin{aligned} \text{and} \quad E\left[|y(t)|^2\right] &= E\left[\sigma_{s1}^2 \left|\mathbf{w}^H \mathbf{a}_1\right|^2\right] + E\left[\sum_{r=2}^q \sigma_{sr}^2 \left|\mathbf{w}^H \mathbf{a}_r\right|^2\right] \\ &\quad + E\left[\sigma_n^2 \mathbf{w}^H \mathbf{w}\right] \equiv P_s + P_i + P_n, \end{aligned} \tag{15}$$

where P_s, P_i, and P_n are the output powers of the desired signal, interference, and noise, respectively. Accordingly, the output SINR of the beamformer $\mathbf{w}$ is given by [5, 11]

$$\text{SINR}(\mathbf{w}) = \frac{P_s}{P_i + P_n}. \tag{16}$$

If the desired signal is received without distortion, i.e., $\mathbf{w}^H \mathbf{a}_1 = 1$, the output SINR of (16) can be further written as

$$\text{SINR}(\mathbf{w}) = \frac{\sigma_{s1}^2}{E\left[\sum_{r=2}^q \sigma_{sr}^2 \left|\mathbf{w}^H \mathbf{a}_r\right|^2\right] + E\left[\sigma_n^2 \mathbf{w}^H \mathbf{w}\right]}. \tag{17}$$

Let $0 < c \equiv p/m < \infty$ denote the ratio between the number of antenna elements and the number of snapshots and assume $\kappa > 0$. It

was presented in [11] that the asymptotic behavior of the output SINR for $\hat{\mathbf{w}}_D$ in (9) is given by

$$\mathrm{SINR}\left(\hat{\mathbf{w}}_D\right) = \left(\frac{u\left(\kappa\right)}{\sigma_{s1}^2} - 1\right)^{-1}, \tag{18}$$

$$\text{where} \quad u\left(\kappa\right) = \frac{1}{1-c\xi} \cdot \frac{\mathbf{a}_1^H \left(\mathbf{R}+\gamma\mathbf{I}\right)^{-1} \mathbf{R} \left(\mathbf{R}+\gamma\mathbf{I}\right)^{-1} \mathbf{a}_1}{\left[\mathbf{a}_1^H \left(\mathbf{R}+\gamma\mathbf{I}\right)^{-1} \mathbf{a}_1\right]^2},$$

$$\xi = \frac{1}{p}\sum_{i=1}^{p}\left(\frac{\lambda_i}{\lambda_i+\gamma}\right)^2, \quad \gamma = \kappa\left(1+cb\right), \tag{19}$$

$\lambda_{\max} = \lambda_1 \geq \lambda_2 \geq \ldots \geq \lambda_p = \lambda_{\min}$ denote the eigenvalues of $\mathbf{R}$, and b in (19) is the unique positive solution to the following equation:

$$b = \frac{1}{p}\sum_{i=1}^{p}\frac{\lambda_i\left(1+cb\right)}{\lambda_i+\kappa\left(1+cb\right)}. \tag{20}$$

Although the expression of (18) is suitable for a general spatial correlation matrix $\mathbf{R}$ and the case with steering vector errors, it is not easy to see how the loading factor κ affects the performance of the array beamformer. To get insights into the output SINR, one might usually resort to computer computations and the plotted curves. The main reason of this drawback is ascribed to the matrix operations in (19), which is hardly been realized by humans. Moreover, it is inconvenient to use (18) since the nonlinear equation in (20) has to be solved. In the next section, we derive the output SINR of $\hat{\mathbf{w}}_D$ based on (9) and attempt to obtain a more explicit expression. Similar to the assumption in [11], the case of positive loading factors is considered in this paper. Negative loading factors are effective for tackling weak interferers on array beamforming [7]. However, the loading factor should be higher than $-\sigma_n^2$ to maintain the positive definite property of the correlation matrix. The more details about negative loading factors can be found in [7, 10].

3. PERFORMANCE OF A MVDR BEAMFORMER WITH DIAGONAL LOADING

Based on the derivation in [5, pp. 929], the weight vector $\hat{\mathbf{w}}$ of the conventional MVDR beamformer in (8) can be derived to

$$\hat{\mathbf{w}} = \frac{\hat{\mathbf{Q}}^{-1}\mathbf{a}_1}{\mathbf{a}_1^H\hat{\mathbf{Q}}^{-1}\mathbf{a}_1} - \hat{\mathbf{P}}\hat{\mathbf{Q}}^{-1}\hat{\mathbf{r}}, \tag{21}$$

where $\hat{\mathbf{P}} = \mathbf{I} - \hat{\mathbf{Q}}^{-1}\mathbf{a}_1\mathbf{a}_1^H/(\mathbf{a}_1^H\hat{\mathbf{Q}}^{-1}\mathbf{a}_1)$ is a projection matrix. Equation (21) shows that $\hat{\mathbf{w}}$ can be expressed by the sum of a MVDR weight vector $\hat{\mathbf{w}}_Q \equiv \hat{\mathbf{Q}}^{-1}\mathbf{a}_1/\mathbf{a}_1^H\hat{\mathbf{Q}}^{-1}\mathbf{a}_1$ without desired signal in the received data vector and a term related to the cross correlation $\hat{\mathbf{r}}$ between the desired signal and undesired component. According to the analysis in [2], the output SINR difference of $\hat{\mathbf{w}}_Q$ and $\mathbf{w}_o$ is within 3 dB when the number of samples is larger than twice of the number of elements. Then, Anu and Wax [5, pp. 929-930] extended this result and claimed that the $\hat{\mathbf{r}}$ in (21) captures the most finite sample effect as compared with the other random quantities $\hat{\mathbf{Q}}$ and $\hat{\mathbf{P}}$. For a moderate sample size $m > 3p$, it is also shown in [5, Eq. (21)] that $\hat{\mathbf{w}}$ in (21) can be approximated by

$$\hat{\mathbf{w}} \approx \frac{\mathbf{Q}^{-1}\mathbf{a}_1}{\mathbf{a}_1^H\mathbf{Q}^{-1}\mathbf{a}_1} - \mathbf{P}\mathbf{Q}^{-1}\hat{\mathbf{r}} \equiv \mathbf{w}_o + \hat{\mathbf{w}}_c, \tag{22}$$

where $\mathbf{P} = \mathbf{I} - \mathbf{Q}^{-1}\mathbf{a}_1\mathbf{a}_1^H/\mathbf{a}_1^H\mathbf{Q}^{-1}\mathbf{a}_1$ and $\hat{\mathbf{w}}_c$ represents the redundant weight vector due to finite samples. Analogous to the $\hat{\mathbf{w}}$ in (21), $\hat{\mathbf{w}}_D$ in (9) can be derived to

$$\hat{\mathbf{w}}_D = \frac{\hat{\mathbf{Q}}_D^{-1}\mathbf{a}_1}{\mathbf{a}_1^H\hat{\mathbf{Q}}_D^{-1}\mathbf{a}_1} - \hat{\mathbf{P}}_D\hat{\mathbf{Q}}_D^{-1}\hat{\mathbf{r}}, \quad \hat{\mathbf{P}}_D = \mathbf{I} - \frac{\hat{\mathbf{Q}}_D^{-1}\mathbf{a}_1\mathbf{a}_1^H}{\mathbf{a}_1^H\hat{\mathbf{Q}}_D^{-1}\mathbf{a}_1}. \tag{23}$$

Applying the approximation $\hat{\mathbf{Q}} \approx \mathbf{Q}$ in (22) and assuming a positive loading factor, we have $\hat{\mathbf{Q}}_D = \hat{\mathbf{Q}} + \kappa \cdot \mathbf{I} \approx \mathbf{Q} + \kappa \cdot \mathbf{I} \equiv \mathbf{Q}_D$ and the approximated $\hat{\mathbf{w}}_D$ given by

$$\hat{\mathbf{w}}_D \approx \frac{\mathbf{Q}_D^{-1}\mathbf{a}_1}{\mathbf{a}_1^H\mathbf{Q}_D^{-1}\mathbf{a}_1} - \mathbf{P}_D\mathbf{Q}_D^{-1}\hat{\mathbf{r}} \equiv \mathbf{w}_D + \hat{\mathbf{w}}_{c,D}, \quad \mathbf{P}_D = \mathbf{I} - \frac{\mathbf{Q}_D^{-1}\mathbf{a}_1\mathbf{a}_1^H}{\mathbf{a}_1^H\mathbf{Q}_D^{-1}\mathbf{a}_1}, \tag{24}$$

where $\mathbf{w}_D = \mathbf{w}_o$ and $\hat{\mathbf{w}}_{c,D} = \hat{\mathbf{w}}_c$ for $\kappa = 0$. To confirm the validity of the approximation used in (24), four examples for the output SINR computed by (9), (23), and (24) versus number of snapshots are presented in Figure 1. An eight-element uniform linear array (ULA) with half-wavelength spacing is considered, and the four different settings for source powers σ_{si}^2, directions θ_i, and loading factors κ are indicated with different colors. Note that the results corresponding to different number of snapshots are computed with independent data samples. As we see from Figure 1, the approximation used in (24) leads to acceptable errors but still preserves the most finite sample effect even if the output SINRs have not reached to their steady-state. To facilitate and simplify the analysis, we adopt this approximation in the following derivations. It was reported in [5] and [12] that the $\hat{\mathbf{w}}_c$ in (22) deteriorates the performance of the conventional MVDR beamformer. In the following analysis, we will explore how the loading

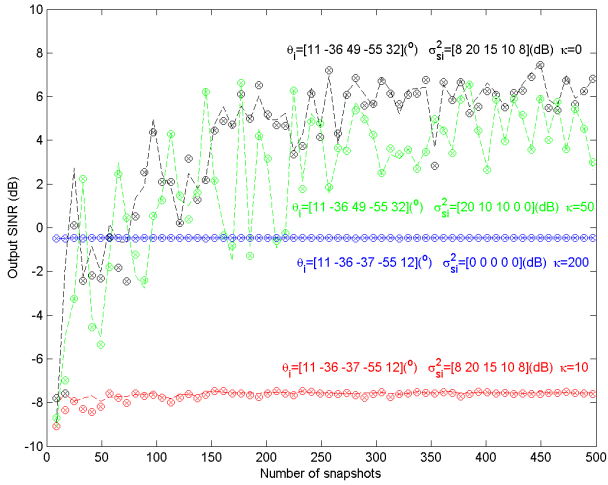

Figure 1. The simulated output SINR versus number of snapshots. '$\circ$': using the $\hat{\mathbf{w}}_D$ in (9). '$\times$': using the $\hat{\mathbf{w}}_D$ in (23). '$--$': using the $\hat{\mathbf{w}}_D$ in (24).

factor mitigates the degradation due to $\hat{\mathbf{w}}_c$. The influence of modifying $\mathbf{w}_o$ to $\mathbf{w}_D$ when $\kappa \neq 0$ will be discussed as well.

3.1. Expressing Output SINR in Terms of Q and Q_D

After some algebra manipulations, it can be shown easily that the approximated $\hat{\mathbf{w}}_D$ of (24) satisfies the unit-gain constraint in the look direction. Therefore, the output SINR of a MVDR beamformer with diagonal loading can be obtained from (17) as follows:

$$\text{SINR}\,(\hat{\mathbf{w}}_D) = \frac{\sigma_{s1}^2}{P_{i,D}+P_{n,D}} = \frac{\sigma_{s1}^2}{E\left[\sum_{r=2}^{q}\sigma_{sr}^2\left|\hat{\mathbf{w}}_D^H\mathbf{a}_r\right|^2\right]+E\left[\sigma_n^2\hat{\mathbf{w}}_D^H\hat{\mathbf{w}}_D\right]}. \quad (25)$$

Using (24) and the property of $\hat{\mathbf{r}}$ in (12), the interference output power $P_{i,D}$ is given by

$$P_{i,D} \approx \sum_{r=2}^{q}\sigma_{sr}^2\left|\mathbf{w}_D^H\mathbf{a}_r\right|^2 + \sum_{r=2}^{q}\sigma_{sr}^2 E\left[\left|\hat{\mathbf{w}}_{c,D}^H\mathbf{a}_r\right|^2\right] \equiv P_{id}+P_{ic}, \quad (26)$$

where P_{id} and P_{ic} are the interference output powers associated with $\mathbf{w}_D$ and $\hat{\mathbf{w}}_{c,D}$, respectively. Using $\mathbf{w}_D$ and $\hat{\mathbf{w}}_{c,D}$ of (24) and the

property of $\hat{\mathbf{r}}$ given by (13), we have

$$P_{id} = \sum_{r=2}^{q} \sigma_{sr}^2 \left| \frac{\mathbf{a}_1^H \mathbf{Q}_D^{-1} \mathbf{a}_r}{\mathbf{a}_1^H \mathbf{Q}_D^{-1} \mathbf{a}_1} \right|^2 \tag{27}$$

$$\text{and} \quad P_{ic} = \sum_{r=2}^{q} \sigma_{sr}^2 E\left[\left| \hat{\mathbf{r}}^H \mathbf{Q}_D^{-1} \mathbf{P}_D^H \mathbf{a}_r \right|^2 \right] = \frac{\sigma_{s1}^2}{m} \sum_{r=2}^{q} \sigma_{sr}^2 \mathbf{a}_r^H \mathbf{P}_D \mathbf{Q}_D^{-1} \mathbf{Q} \mathbf{Q}_D^{-1} \mathbf{P}_D^H \mathbf{a}_r. \tag{28}$$

Similar to the calculation in (26)–(28), we have the noise output power $P_{n,D}$ given as follows:

$$P_{n,D} \approx \sigma_n^2 \mathbf{w}_D^H \mathbf{w}_D + \sigma_n^2 E\left[\hat{\mathbf{w}}_{c,D}^H \hat{\mathbf{w}}_{c,D} \right] \equiv P_{nd} + P_{nc}, \tag{29}$$

$$P_{nd} = \sigma_n^2 \frac{\left\| \mathbf{Q}_D^{-1} \mathbf{a}_1 \right\|^2}{\left(\mathbf{a}_1^H \mathbf{Q}_D^{-1} \mathbf{a}_1 \right)^2}, \tag{30}$$

$$\text{and} \quad P_{nc} = \sigma_n^2 tr\left(\mathbf{Q}_D^{-1} \mathbf{P}_D^H \mathbf{P}_D \mathbf{Q}_D^{-1} E\left[\hat{\mathbf{r}} \hat{\mathbf{r}}^H \right] \right) = \frac{\sigma_{s1}^2 \sigma_n^2}{m} tr\left(\mathbf{Q}_D^{-1} \mathbf{P}_D^H \mathbf{P}_D \mathbf{Q}_D^{-1} \mathbf{Q} \right), \tag{31}$$

where $||\cdot||$ and $tr(\cdot)$ are the Euclidean norm of a vector and the trace of a matrix, respectively. Note that P_{id}, P_{nd}, P_{ic}, and P_{nc} are all positive by definition. Using the expression of $\mathbf{Q}$ in (3), the relationship $\mathbf{Q}_D^{-1} \mathbf{P}_D^H = \mathbf{P}_D \mathbf{Q}_D^{-1}$, and $\mathbf{P}_D$ of (24), the interference-plus-noise output power $P_{ic} + P_{nc}$ due to $\hat{\mathbf{w}}_{c,D}$ can be written as

$$P_{ic} + P_{nc} = \frac{\sigma_{s1}^2}{m} \left[tr\left(\mathbf{Q}_D^{-1} \mathbf{Q} \mathbf{Q}_D^{-1} \mathbf{Q} \right) - 2 \frac{\mathbf{a}_1^H \mathbf{Q}_D^{-1} \mathbf{Q} \mathbf{Q}_D^{-1} \mathbf{Q} \mathbf{Q}_D^{-1} \mathbf{a}_1}{\mathbf{a}_1^H \mathbf{Q}_D^{-1} \mathbf{a}_1} + \left(\frac{\mathbf{a}_1^H \mathbf{Q}_D^{-1} \mathbf{Q} \mathbf{Q}_D^{-1} \mathbf{a}_1}{\mathbf{a}_1^H \mathbf{Q}_D^{-1} \mathbf{a}_1} \right)^2 \right]. \tag{32}$$

Substituting (26), (27), (29), (30), and (32) into (25), we have an approximated formula for $\text{SINR}\left(\hat{\mathbf{w}}_D\right)$ in terms of $\mathbf{Q}$ and $\mathbf{Q}_D$ given by

$$\text{SINR}\left(\hat{\mathbf{w}}_D\right) \approx \frac{\sigma_{s1}^2}{P_{id} + P_{nd} + P_{ic} + P_{nc}} = \sigma_{s1}^2 \left[\begin{array}{l} \sum_{r=2}^{q} \sigma_{sr}^2 \left| \frac{\mathbf{a}_1^H \mathbf{Q}_D^{-1} \mathbf{a}_r}{\mathbf{a}_1^H \mathbf{Q}_D^{-1} \mathbf{a}_1} \right|^2 + \sigma_n^2 \frac{\left\| \mathbf{Q}_D^{-1} \mathbf{a}_1 \right\|^2}{\left(\mathbf{a}_1^H \mathbf{Q}_D^{-1} \mathbf{a}_1 \right)^2} + \frac{\sigma_{s1}^2}{m} tr\left(\mathbf{Q}_D^{-1} \mathbf{Q} \mathbf{Q}_D^{-1} \mathbf{Q} \right) \\ -2 \frac{\sigma_{s1}^2}{m} \cdot \frac{\mathbf{a}_1^H \mathbf{Q}_D^{-1} \mathbf{Q} \mathbf{Q}_D^{-1} \mathbf{Q} \mathbf{Q}_D^{-1} \mathbf{a}_1}{\mathbf{a}_1^H \mathbf{Q}_D^{-1} \mathbf{a}_1} + \frac{\sigma_{s1}^2}{m} \left(\frac{\mathbf{a}_1^H \mathbf{Q}_D^{-1} \mathbf{Q} \mathbf{Q}_D^{-1} \mathbf{a}_1}{\mathbf{a}_1^H \mathbf{Q}_D^{-1} \mathbf{a}_1} \right)^2 \end{array} \right]^{-1}. \tag{33}$$

In contrast to (18), Equation (33) provides a straightforward closed-form to the output SINR of a MVDR beamformer with diagonal loading. Especially, no cumbersome nonlinear equation has to be solved before using (33), which prevents the potential possibility of computational burden. However, one should notice that the formula in (33) is valid only when the approximation used in (24) is a reasonable one. The output SINRs of $\hat{\mathbf{w}}$ (the conventional MVDR beamformer) and $\mathbf{w}_D$ (the diagonal-loaded MVDR beamformer without finite sample effect) can be obtained by substituting $\kappa = 0$ ($\mathbf{Q}_D = \mathbf{Q}$) and $m \to \infty$, respectively, into (33) as follows:

$$\mathrm{SINR}(\hat{\mathbf{w}}) \approx \frac{\sigma_{s1}^2}{\sum_{r=2}^{q} \sigma_{sr}^2 \left| \frac{\mathbf{a}_1^H \mathbf{Q}^{-1} \mathbf{a}_r}{\mathbf{a}_1^H \mathbf{Q}^{-1} \mathbf{a}_1} \right|^2 + \sigma_n^2 \frac{\|\mathbf{Q}^{-1}\mathbf{a}_1\|^2}{\left(\mathbf{a}_1^H \mathbf{Q}^{-1} \mathbf{a}_1\right)^2} + \frac{(p-1)\sigma_{s1}^2}{m}}, \quad (34)$$

$$\mathrm{SINR}(\mathbf{w}_D) \approx \sigma_{s1}^2 \left[\sum_{r=2}^{q} \sigma_{sr}^2 \left| \frac{\mathbf{a}_1^H \mathbf{Q}_D^{-1} \mathbf{a}_r}{\mathbf{a}_1^H \mathbf{Q}_D^{-1} \mathbf{a}_1} \right|^2 + \sigma_n^2 \frac{\left\|\mathbf{Q}_D^{-1}\mathbf{a}_1\right\|^2}{\left(\mathbf{a}_1^H \mathbf{Q}_D^{-1} \mathbf{a}_1\right)^2} \right]^{-1}. \quad (35)$$

3.2. Output SINR Expression for Two Interferers

In spite of the advantages over (18), it is not easy to realize the influence of system parameters and loading factors on the output SINR from (33) due to the matrix manipulations. To get more insights into $\mathrm{SINR}(\hat{\mathbf{w}}_D)$, we further expand $\mathbf{Q}$ and $\mathbf{Q}_D^{-1}$ in this section. However, the number q of sources should be specified for further derivation. Here, we consider q= 3 and derive P_{id}, P_{nd}, and $P_{ic} + P_{nc}$, respectively.

For $q = 3$, $\mathbf{Q}$ and $\mathbf{Q}_D$ are reduced to

$$\mathbf{Q} = \sigma_{s2}^2 \mathbf{a}_2 \mathbf{a}_2^H + \sigma_{s3}^2 \mathbf{a}_3 \mathbf{a}_3^H + \sigma_n^2 \mathbf{I} \quad (36)$$

$$\text{and} \quad \mathbf{Q}_D = \sigma_{s2}^2 \mathbf{a}_2 \mathbf{a}_2^H + \sigma_{s3}^2 \mathbf{a}_3 \mathbf{a}_3^H + \tilde{\sigma}_n^2 \mathbf{I}, \quad (37)$$

where $\tilde{\sigma}_n^2 \equiv \sigma_n^2 + \kappa$. Letting $d_{ij} \equiv \mathbf{a}_i^H \mathbf{a}_j / p$ for $i < j$ and applying the matrix inversion lemma twice, we get the following expression for $\mathbf{Q}_D^{-1}$:

$$\mathbf{Q}_D^{-1} = \frac{\left[\begin{array}{l} \tilde{\sigma}_n^4 \mathbf{I} + \sigma_{s2}^2 \tilde{\sigma}_n^2 \left(p\mathbf{I} - \mathbf{a}_2 \mathbf{a}_2^H\right) + \sigma_{s3}^2 \tilde{\sigma}_n^2 \left(p\mathbf{I} - \mathbf{a}_3 \mathbf{a}_3^H\right) \\ + \sigma_{s2}^2 \sigma_{s3}^2 \left(p^2 z_b \mathbf{I} - p\mathbf{Z}_a\right) \end{array} \right]}{\tilde{\sigma}_n^2 \left(\tilde{\sigma}_n^4 + p\sigma_{s2}^2 \tilde{\sigma}_n^2 + p\sigma_{s3}^2 \tilde{\sigma}_n^2 + p^2 \sigma_{s2}^2 \sigma_{s3}^2 z_b\right)}, \quad (38)$$

where $\mathbf{Z}_a \equiv \mathbf{a}_2 \mathbf{a}_2^H + \mathbf{a}_3 \mathbf{a}_3^H - d_{23}^* \mathbf{a}_3 \mathbf{a}_2^H - d_{23} \mathbf{a}_2 \mathbf{a}_3^H$, $z_b \equiv 1 - |d_{23}|^2$ are defined for simplicity, and $\{\cdot\}^*$ denotes complex conjugate. Using the expression of $\mathbf{Q}_D^{-1}$ in (38), it is straightforward to obtain the expressions for $\mathbf{a}_1^H \mathbf{Q}_D^{-1} \mathbf{a}_1$, $\mathbf{a}_1^H \mathbf{Q}_D^{-1} \mathbf{a}_2$, $\mathbf{a}_1^H \mathbf{Q}_D^{-1} \mathbf{a}_3$, and $||\mathbf{Q}_D^{-1} \mathbf{a}_1||^2$ presented in Appendix A. When the angular separation for each pair

of the incident signal sources is larger than a beamwidth and the inter-element spacing of the array is appropriate, we can assume that $|d_{ij}|^2 \ll 1$ for $i \neq j$ [4, 31], which implies the adaptive array is capable of differentiating the signal sources in the environment normally. Applying this assumption and substituting (A1)–(A4) into the P_{id} and P_{nd} of (33) yields

$$P_{id} \approx \frac{\sigma_{s2}^2 \left(\sigma_n^2+\kappa\right)^2 |d_{12}|^2}{\left(\sigma_n^2+\kappa+p\sigma_{s2}^2\right)^2} + \frac{\sigma_{s3}^2 \left(\sigma_n^2+\kappa\right)^2 |d_{13}|^2}{\left(\sigma_n^2+\kappa+p\sigma_{s3}^2\right)^2} \quad (39)$$

$$\text{and} \quad P_{nd} \approx \frac{\sigma_n^2}{p}. \quad (40)$$

Next, we derive $P_{ic}+P_{nc}$ under $q=3$. For simplicity, let the three terms in $P_{ic}+P_{nc}$ of (32) be defined as

$$\Omega_1 \equiv tr\left(\mathbf{Q}_D^{-1}\mathbf{Q}\mathbf{Q}_D^{-1}\mathbf{Q}\right), \quad \Omega_2 \equiv \frac{\mathbf{a}_1^H\mathbf{Q}_D^{-1}\mathbf{Q}\mathbf{Q}_D^{-1}\mathbf{Q}\mathbf{Q}_D^{-1}\mathbf{a}_1}{\mathbf{a}_1^H\mathbf{Q}_D^{-1}\mathbf{a}_1},$$

$$\text{and} \quad \Omega_3 \equiv \frac{\mathbf{a}_1^H\mathbf{Q}_D^{-1}\mathbf{Q}\mathbf{Q}_D^{-1}\mathbf{a}_1}{\mathbf{a}_1^H\mathbf{Q}_D^{-1}\mathbf{a}_1}. \quad (41)$$

Utilizing $\mathbf{Q}_D^{-1}$ in (38) and $\mathbf{Q}$ in (36) and performing some algebraic manipulations, we have $\mathbf{Q}_D^{-1}\mathbf{Q}$ and $\mathbf{Q}_D^{-1}\mathbf{Q}\mathbf{Q}_D^{-1}\mathbf{Q}$ shown in Appendix A. Based on (36)–(38), (A1)–(A6) and after some lengthy algebraic manipulations, it is straightforward to derive the expressions for Ω_1, Ω_2, and Ω_3. Similarly, using $|d_{ij}|^2 \ll 1$ for $i \neq j$, we obtain the approximated Ω_1, Ω_2, and Ω_3 given by (A7)–(A9). Combining the terms in the square bracket of (32) and neglecting the higher order terms of d_{ij} for $i \neq j$, we have the approximated $P_{ic}+P_{nc}$ given by

$$P_{ic}+P_{nc} \approx \frac{\sigma_{s1}^2}{m}\left[\begin{array}{l}\sum\limits_{r=2}^{3} \frac{\kappa p\sigma_{sr}^2}{(\sigma_n^2+\kappa)(p\sigma_{sr}^2+\sigma_n^2+\kappa)}\left(\frac{\sigma_n^2}{\sigma_n^2+\kappa}+\frac{p\sigma_{sr}^2+\sigma_n^2}{p\sigma_{sr}^2+\sigma_n^2+\kappa}\right) \\ +\frac{2p^2\sigma_{s2}^2\sigma_{s3}^2\left(\sigma_n^2+\kappa\right)^2|d_{23}|^2}{\left(p\sigma_{s2}^2+\sigma_n^2+\kappa\right)^2\left(p\sigma_{s3}^2+\sigma_n^2+\kappa\right)^2}+\frac{\sigma_n^4}{\left(\sigma_n^2+\kappa\right)^2}(p-1)\end{array}\right]. \quad (42)$$

Moreover, it is shown in Appendix B that the term $2p^2\sigma_{s2}^2\sigma_{s3}^2(\sigma_n^2+\kappa)^2|d_{23}|^2/[(p\sigma_{s2}^2+\sigma_n^2+\kappa)^2(p\sigma_{s3}^2+\sigma_n^2+\kappa)^2]$ in the square bracket is marginal and can be neglected when assuming $2|d_{23}|^2 \ll 1$. Hence, an appropriate approximation for $P_{ic}+P_{nc}$ is given as follows:

$$P_{ic}+P_{nc} \approx \frac{\sigma_{s1}^2}{m}\frac{\sigma_n^4}{\left(\sigma_n^2+\kappa\right)^2}(p-1)$$

$$+\frac{\sigma_{s1}^2}{m}\sum_{r=2}^{3}\frac{\kappa p\sigma_{sr}^2}{\left(\sigma_n^2+\kappa\right)\left(p\sigma_{sr}^2+\sigma_n^2+\kappa\right)}\left(\frac{\sigma_n^2}{\sigma_n^2+\kappa}+\frac{p\sigma_{sr}^2+\sigma_n^2}{p\sigma_{sr}^2+\sigma_n^2+\kappa}\right). \quad (43)$$

Based on the derived results in (39), (40), and (43), we obtain the approximated $\mathrm{SINR}\left(\hat{\mathbf{w}}_D\right)$ for $q=3$ given by

$$\begin{aligned}\mathrm{SINR}\left(\hat{\mathbf{w}}_D\right)|_{q=3} &\approx \frac{\sigma_{s1}^2}{P_{id}+P_{nd}+P_{ic}+P_{nc}} \\ &\approx \sigma_{s1}^2\left[\begin{array}{l}\sum\limits_{r=2}^{3}\frac{\sigma_{sr}^2\left(\sigma_n^2+\kappa\right)^2|d_{1r}|^2}{\left(\sigma_n^2+\kappa+p\sigma_{sr}^2\right)^2}+\frac{\sigma_n^2}{p}+\frac{\sigma_{s1}^2}{m}\cdot\frac{\sigma_n^4}{\left(\sigma_n^2+\kappa\right)^2}(p-1) \\ +\frac{\sigma_{s1}^2}{m}\sum\limits_{r=2}^{3}\frac{\kappa p\sigma_{sr}^2}{\left(\sigma_n^2+\kappa\right)\left(p\sigma_{sr}^2+\sigma_n^2+\kappa\right)}\left(\frac{\sigma_n^2}{\sigma_n^2+\kappa}+\frac{p\sigma_{sr}^2+\sigma_n^2}{p\sigma_{sr}^2+\sigma_n^2+\kappa}\right)\end{array}\right]^{-1}. \quad (44)\end{aligned}$$

Since the output SINR in (44) is expressed in terms of system parameters and loading factors, it provides more insights and is more comprehensive than the expression in (18) or (33). The explicit formula facilitates the analysis of distinct factors in the performance of MVDR beamformers. Similar to (33)–(35), the more explicit formula for $\hat{\mathbf{w}}$ and $\mathbf{w}_D$ can be obtained by substituting $\kappa=0$ and $m\to\infty$, respectively, into (44) as follows:

$$\mathrm{SINR}\left(\hat{\mathbf{w}}\right)|_{q=3} \approx \sigma_{s1}^2\left[\sum_{r=2}^{3}\frac{\sigma_{sr}^2\sigma_n^4\left|d_{1r}\right|^2}{\left(\sigma_n^2+p\sigma_{sr}^2\right)^2}+\frac{\sigma_n^2}{p}+\frac{\sigma_{s1}^2}{m}(p-1)\right]^{-1}, \quad (45)$$

$$\mathrm{SINR}\left(\mathbf{w}_D\right)|_{q=3} \approx \sigma_{s1}^2\left[\sum_{r=2}^{3}\frac{\sigma_{sr}^2\left(\sigma_n^2+\kappa\right)^2\left|d_{1r}\right|^2}{\left(\sigma_n^2+\kappa+p\sigma_{sr}^2\right)^2}+\frac{\sigma_n^2}{p}\right]^{-1}. \quad (46)$$

For convenience, the derived formulas and corresponding assumptions are summarized in Table 1.

Table 1. The summary of the derived output SINR formulas.

	$\mathrm{SINR}\left(\mathbf{w}_D\right)$	$\mathrm{SINR}\left(\hat{\mathbf{w}}_D\right)$	Assumptions
SINR in terms of $\mathbf{Q}$ and $\mathbf{Q}_D$	(35)	(33)	1. $2\le q<p$ 2. $\hat{\mathbf{w}}_D\approx\mathbf{w}_D+\hat{\mathbf{w}}_{c,D}$
Explicit SINR for $q=3$	(46)	(44)	1. $q=3$ 2. $\hat{\mathbf{w}}_D\approx\mathbf{w}_D+\hat{\mathbf{w}}_{c,D}$ 3. $\lvert d_{ij}\rvert^2\ll 1$ for $\mathrm{SINR}\left(\mathbf{w}_D\right)$ $2\lvert d_{ij}\rvert^2\ll 1$ for $\mathrm{SINR}\left(\hat{\mathbf{w}}_D\right)$
Explicit SINR for general q	(61)	(62)	1. $2\le q<p$ 2. $\hat{\mathbf{w}}_D\approx\mathbf{w}_D+\hat{\mathbf{w}}_{c,D}$ 3. $\lvert d_{ij}\rvert^2\ll 1$ for $\mathrm{SINR}\left(\mathbf{w}_D\right)$ $2\lvert d_{ij}\rvert^2\ll 1$ for $\mathrm{SINR}\left(\hat{\mathbf{w}}_D\right)$

4. DISCUSSIONS REGARDING THE THEORETICAL RESULTS

In this section, we discuss the influence of the loading factor κ on P_{id} associated with the infinite data performance and $P_{ic} + P_{nc}$ associated with finite sample effect based on the approximated output SINR expression in (44). In addition, the possibility of extending the scope of (44)–(46) to the more general scenario $2 \leq q < p$ is considered in Section 4.3. For simplicity, the "$\approx$" in (44) is replaced by "$=$" in the following discussions.

4.1. The Characteristic of P_{id}

Based on (39), we have

$$P_{id}|_{\kappa\to\infty} = \sum_{r=2}^{3} \sigma_{sr}^2 \left|d_{1r}\right|^2 \tag{47}$$

$$\text{and} \quad P_{id}|_{\kappa=0} = \sum_{r=2}^{3} \frac{\sigma_{sr}^2 \sigma_n^4 \left|d_{1r}\right|^2}{\left(\sigma_n^2 + p\sigma_{sr}^2\right)^2}. \tag{48}$$

The P_{id} in (47) and (48) are the interference output powers of a phased array and a fully adaptive array without finite sample effect, respectively. We note that $P_{id}|_{\kappa=0}$ is always smaller than $P_{id}|_{\kappa\to\infty}$ because of $p\sigma_{sr}^2$. Using (39), the first derivative of P_{id} with respect to κ is given by

$$P'_{id} = 2p \sum_{r=2}^{3} \frac{\sigma_{sr}^4 \left(\sigma_n^2 + \kappa\right) \left|d_{1r}\right|^2}{\left(\sigma_n^2 + \kappa + p\sigma_{sr}^2\right)^3} > 0. \tag{49}$$

Based on the facts of $P_{id}|_{\kappa\to\infty} > P_{id}|_{\kappa=0}$ and $P'_{id} > 0$, it is found that P_{id} is a monotonic increasing function of κ. This reveals that increasing the loading level always leads to a larger P_{id} and is detrimental to the performance of MVDR beamformers. In other words, the infinite data performance in (46) always drops with the growth of the loading level.

Next, we explore the increasing rate of P_{id} with κ by evaluating the upper bound of P'_{id}. First, the second derivative of P_{id} is given by

$$P''_{id} = 2p \sum_{r=2}^{3} \sigma_{sr}^4 \left|d_{1r}\right|^2 \frac{p\sigma_{sr}^2 - 2\sigma_n^2 - 2\kappa}{\left(\sigma_n^2 + \kappa + p\sigma_{sr}^2\right)^4}, \tag{50}$$

which indicates the variation of the slope of P_{id}. Let $P'_{id,r}$ and $P''_{id,r}$, $r = 2, 3$, be the $(r-1)$th term of the summations in (49) and (50), respectively. It is found that $P''_{id,r}$ is greater than zero for κ

lower than $(p\sigma_{sr}^2 - 2\sigma_n^2)/2$, and vice versa. That is, $P'_{id,r}$ increases for $\kappa < (p\sigma_{sr}^2 - 2\sigma_n^2)/2$ and decreases for $\kappa > (p\sigma_{sr}^2 - 2\sigma_n^2)/2$. The maximum $P'_{id,r}$ is located at $\kappa = (p\sigma_{sr}^2 - 2\sigma_n^2)/2$ and is given by

$$\max P'_{id,r} = P'_{id,r}|_{\kappa=(p\sigma_{sr}^2-2\sigma_n^2)/2} = \frac{8\,|d_{1r}|^2}{27p}. \tag{51}$$

Therefore, the upper bound of P'_{id} is

$$\max P'_{id} = \frac{8}{27p}\sum_{r=2}^{3}|d_{1r}|^2. \tag{52}$$

Equation (52) implies that P_{id} increases slowly as κ increases because of the assumption $|d_{1r}|^2 \ll 1$, $r \neq 1$. In summary, increasing the loading level results in a slight growth on P_{id} in (44). Under infinite data samples, the weight vector $\mathbf{w}_D$ can never be the optimal one in the sense of maximum SINR unless $\kappa = 0$.

4.2. The Characteristics of $P_{ic} + P_{nc}$

Using the result of (43), the term $P_{ic} + P_{nc}$ for $\kappa \to \infty$ and $\kappa = 0$ can be derived to

$$P_{ic} + P_{nc}|_{\kappa\to\infty} = 0 \tag{53}$$

and

$$P_{ic} + P_{nc}|_{\kappa=0} = \frac{(p-1)\,\sigma_{s1}^2}{m}, \tag{54}$$

respectively. When the data sample size m is deficient, the $P_{ic}+P_{nc}$ of the conventional MVDR beamformer in (45) may be substantial and degrade the performance. On the other hand, it disappears when the system is reduced to a phased array. Taking the first derivative of $P_{ic} + P_{nc}$ and performing some necessary algebraic manipulations, we obtain

$$\begin{aligned}(P_{ic}+P_{nc})' = {} & \frac{-2\sigma_{s1}^2\sigma_n^4}{m\left(\sigma_n^2+\kappa\right)^3}\left[p-1-\sum_{r=2}^{3}\frac{p\sigma_{sr}^2\left(p\sigma_{sr}^2+\sigma_n^2\right)^2}{\left(p\sigma_{sr}^2+\sigma_n^2+\kappa\right)^3}\right] \\ & -\frac{2p\sigma_{s1}^2}{m}\sum_{r=2}^{3}\frac{\kappa^2\sigma_{sr}^2\left[3\sigma_n^2\left(p\sigma_{sr}^2+\sigma_n^2\right)+\kappa\left(p\sigma_{sr}^2+2\sigma_n^2\right)\right]}{\left(\sigma_n^2+\kappa\right)^3\left(p\sigma_{sr}^2+\sigma_n^2+\kappa\right)^3}.\end{aligned} \tag{55}$$

Obviously, the second term on the right-hand side of (55) is non-positive for $\kappa \geq 0$. Moreover, the assumption of $q = 3 < p$ and the fact $p\sigma_{sr}^2(p\sigma_{sr}^2 + \sigma_n^2)^2/(p\sigma_{sr}^2 + \sigma_n^2 + \kappa)^3 < 1$ make the value of the square bracket in (55) positive. Hence, the first term of (55) is negative, and $P_{ic} + P_{nc}$ is a monotonic decreasing function of κ. This indicates that

$P_{ic}+P_{nc}$ due to finite sample effect can always be reduced by increasing the loading level at the price of increasing P_{id}. To enhance the output SINR, it would be worth increasing κ if the reduction of $P_{ic}+P_{nc}$ is much greater than the growth of P_{id}.

The slopes of $P_{ic}+P_{nc}$ for $\kappa \to \infty$ and $\kappa = 0$ are given by

$$(P_{ic}+P_{nc})'|_{\kappa\to\infty} = 0 \tag{56}$$

$$\text{and} \quad (P_{ic}+P_{nc})'|_{\kappa=0} = \frac{-2\sigma_{s1}^2}{m\sigma_n^2}\left(p-1-\sum_{r=2}^{3}\frac{p\sigma_{sr}^2}{p\sigma_{sr}^2+\sigma_n^2}\right), \tag{57}$$

respectively. From (57), we note that the absolute value of the slope for $\kappa = 0$ is large and $P_{ic}+P_{nc}$ decreases rapidly as κ increases in the case of deficient sample size or strong desired signal power. A small increment of κ would suppress the $P_{ic}+P_{nc}$ of the conventional MVDR beamformer efficiently when the finite sample effect is severe. For $\kappa \to \infty$, both the magnitude and variation of $P_{ic}+P_{nc}$ are equal to zero and hence, there is no finite sample effect on the output SINR because the beamformer becomes a phased array without adaptation. To examine the variation of the slope, we take the second derivative of $P_{ic}+P_{nc}$ as follows:

$$\begin{aligned}(P_{ic}+P_{nc})'' = {} & \frac{6\sigma_{s1}^2\sigma_n^4}{m\left(\sigma_n^2+\kappa\right)^4}\left[(p-1)-\sum_{r=2}^{3}\frac{p\sigma_{sr}^2\delta_r^2\left(4\kappa+\delta_r+\sigma_n^2\right)}{\left(\delta_r+\kappa\right)^4}\right] \\ & +\frac{6p\sigma_{s1}^2}{m}\sum_{r=2}^{3}\frac{\sigma_{sr}^2\left(4\kappa^3\delta_r\sigma_n^2+\kappa^4\sigma_n^2+\kappa^4\delta_r\right)}{\left(\sigma_n^2+\kappa\right)^4\left(\delta_r+\kappa\right)^4},\end{aligned} \tag{58}$$

where $\delta_r \equiv p\sigma_{sr}^2+\sigma_n^2 > 0$. The second term on the right-hand side of (58) is nonnegative. After some algebraic manipulations, it can be proved that each term of the summation in the square bracket of the first term must be lower than 1. Similar to the condition in (55), the first term on the right-hand side of (58) is positive since $q = 3 < p$. Therefore, the second derivative of $P_{ic}+P_{nc}$ is positive, and the slope of $P_{ic}+P_{nc}$ increases monotonically when κ increases from zero to positive infinity. This fact implies the efficiency of eliminating $P_{ic}+P_{nc}$ by increasing loading level is getting lower and lower. As a result, applying a modest positive loading factor to a MVDR beamformer can eliminate the $P_{ic}+P_{nc}$ due to finite sample effect efficiently at the price of slight growth of P_{id}. However, excessive loading level may lead to a larger P_{id} and depress the performance contrarily. A good choice of the loading factor κ should lie in the range where $P_{ic}+P_{nc}$ has been reduced greatly and P_{id} has not become significant yet.

4.3. Generalize the Explicit Expressions to the q-sources Scenario

It is possible to generalize the formula of (46) from $q = 3$ to any $2 \leq q < p$. The SINR($\mathbf{w}_D$) for $q = 2$ and 1 can be obtained readily by substituting $\sigma_{s3}^2 = 0$ and $\sigma_{s2}^2 = \sigma_{s3}^2 = 0$ into (46), respectively, as follows:

$$\mathrm{SINR}\left(\mathbf{w}_D\right)|_{q=2} \approx \sigma_{s1}^2 \left[\frac{\sigma_{s2}^2 \left(\sigma_n^2 + \kappa\right)^2 |d_{12}|^2}{\left(\sigma_n^2 + \kappa + p\sigma_{s2}^2\right)^2} + \frac{\sigma_n^2}{p} \right]^{-1}, \tag{59}$$

$$\mathrm{SINR}\left(\mathbf{w}_D\right)|_{q=1} \approx \sigma_{s1}^2 \left[\frac{\sigma_n^2}{p} \right]^{-1}. \tag{60}$$

From (46), (59), and (60), we find that one term is produced in P_{id} once an interferer is added. Based on this regularity, the approximated formula of SINR($\mathbf{w}_D$) for any $2 \leq q < p$ could be generalized as follows:

$$\mathrm{SINR}\left(\mathbf{w}_D\right) \approx \frac{\sigma_{s1}^2}{P_{id} + P_{nd}} \approx \sigma_{s1}^2 \left[\sum_{r=2}^{q} \frac{\sigma_{sr}^2 \left(\sigma_n^2+\kappa\right)^2 |d_{1r}|^2}{\left(\sigma_n^2+\kappa+p\sigma_{sr}^2\right)^2} + \frac{\sigma_n^2}{p} \right]^{-1}. \tag{61}$$

Note that the restriction of $q < p$ is required to satisfy $|d_{ij}|^2 \ll 1$ for $i \neq j$, which was used to derive (46). It is proved by mathematical induction [32, 33] in Appendix C that the P_{id} and P_{nd} in (33) or (35) are approximately equal to those in (61), respectively, which confirms the validity of (61).

Similar to the extension of SINR($\mathbf{w}_D$) above, the SINR$\left(\hat{\mathbf{w}}_D\right)$ in (44) could be generalized to the scenario of $2 \leq q < p$ as follows:

$$\begin{aligned} \mathrm{SINR}\left(\hat{\mathbf{w}}_D\right) &\approx \frac{\sigma_{s1}^2}{P_{id} + P_{nd} + P_{ic} + P_{nc}} \\ &\approx \sigma_{s1}^2 \left[\begin{array}{l} \sum\limits_{r=2}^{q} \frac{\sigma_{sr}^2\left(\sigma_n^2+\kappa\right)^2|d_{1r}|^2}{\left(\sigma_n^2+\kappa+p\sigma_{sr}^2\right)^2} + \frac{\sigma_n^2}{p} + \frac{\sigma_{s1}^2}{m} \cdot \frac{\sigma_n^4}{\left(\sigma_n^2+\kappa\right)^2}(p-1) \\ + \frac{\sigma_{s1}^2}{m} \sum\limits_{r=2}^{q} \frac{\kappa p \sigma_{sr}^2}{\left(\sigma_n^2+\kappa\right)\left(p\sigma_{sr}^2+\sigma_n^2+\kappa\right)} \left(\frac{\sigma_n^2}{\sigma_n^2+\kappa} + \frac{p\sigma_{sr}^2+\sigma_n^2}{p\sigma_{sr}^2+\sigma_n^2+\kappa} \right) \end{array} \right]^{-1}. \end{aligned} \tag{62}$$

In contrast to the implicit formula presented in (18), the output SINR expression in (62) shows the influence of different parameters on the performance explicitly. According to our investigation, it is not an easy task to show that the $P_{ic}+P_{nc}$ in (62) can be derived from the $P_{ic}+P_{nc}$ in (33) by mathematical induction. Instead of the mathematical proof, we confirm the validity of generalizing $P_{ic} + P_{nc}$ experimentally in the next section. As we will see from the simulations, the formula in (62) usually meets the actual output SINR well for $q > 3$. Besides, the results computed by (62) are sometimes more accurate than those computed by (18).

5. SIMULATION RESULTS

In this section, we present an example to confirm the validity of the theoretical work. In this example, an eight-element ULA with half-wavelength spacing is considered. The noise is complex white Gaussian with zero mean and unit variance ($\sigma_n^2 = 1$). Seven zero mean complex Gaussian signal sources with variances $\sigma_{s1}^2 \sim \sigma_{s7}^2 = [5\,10\,10\,8\,15\,20\,20]$ (dB) and incident angles $\theta_1 \sim \theta_7 = [20^\circ\,40^\circ\,60^\circ\,-3^\circ\,-30^\circ\,-35^\circ\,-50^\circ]$ off broadside are of interest in the following demonstration, where the first one characterizes the single desired signal. The default settings for the number of snapshots and the loading factor are 30 and 10 (i.e., 10 dB above noise power), respectively. For all simulation results, the output SINRs obtained from data samples are computed by (17) where the mathematical expectation is replaced by the sample-average of 100 Monte Carlo trials. The theoretical results computed according to (62) and (18) are presented for comparison.

First, we consider the case of $q = 3$ and examine the accuracy of (44). The output SINR versus loading factor is shown in Figure 2. The theoretical results computed by (44) are closer to the simulated ones for $\kappa < 60$, while (18) provides more accurate results in the other range. In spite of the bias for $\kappa > 60$, the differences between (44) and the simulated results are within 0.5 dB. The curves of the output SINR in Figure 2 are sharp when κ approaches zero. It achieves its maximum for $\kappa \approx 50$ and then drops gradually. This phenomenon

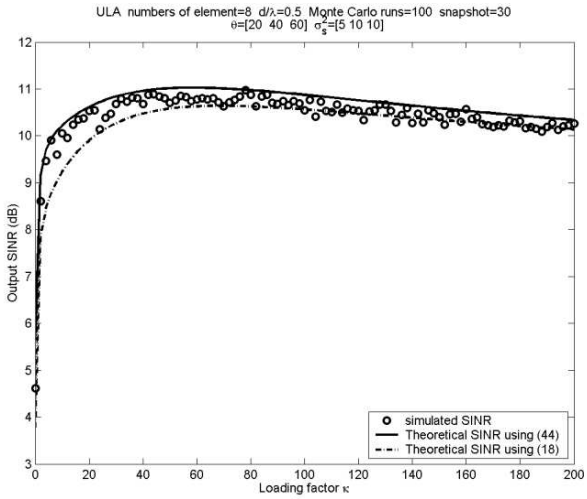

Figure 2. The output SINR versus loading factor for $q = 3$.

can be explained by the theoretical terms P_{id}, P_{nd}, and $P_{ic} + P_{nc}$ plotted in Figure 3. As we expected from the theoretical work in Sections 4.1 and 4.2, P_{id} is a monotonically increasing function of κ with a small increasing rate, and $P_{ic}+P_{nc}$ is a monotonically decreasing one with a large decreasing rate for smaller κ's. Since P_{id} is almost invariant as compared with $P_{ic}+P_{nc}$ for κ approaching zero, the output

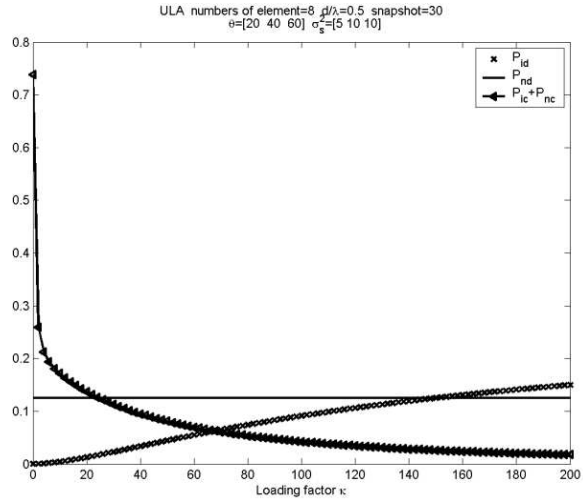

Figure 3. The theoretical terms versus loading factor for $q = 3$.

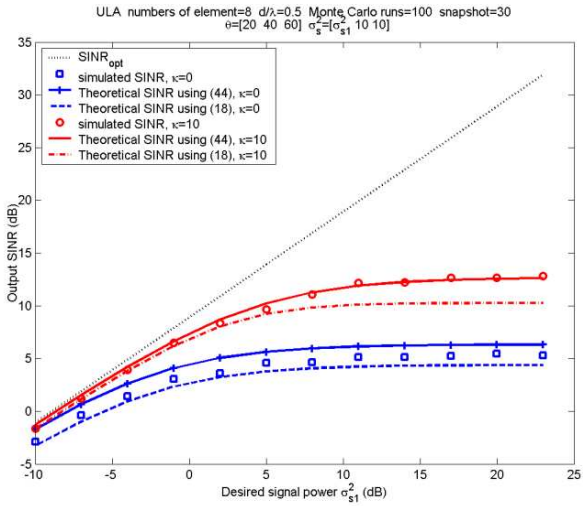

Figure 4. The output SINR versus desired signal power for $q = 3$.

SINR is dominated by $P_{ic} + P_{nc}$ and increased rapidly. However, the increasing P_{id} deteriorates the array performance when $P_{ic} + P_{nc}$ has been reduced to a small level. An appropriate loading factor offering desirable performance should be in the region where $P_{ic}+P_{nc}$ has been suppressed greatly and P_{id} has not become significant yet. For κ equal

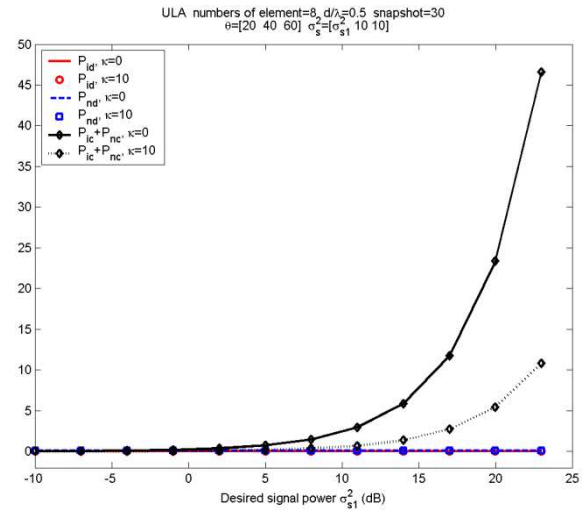

Figure 5. The theoretical terms versus desired signal power for $q = 3$.

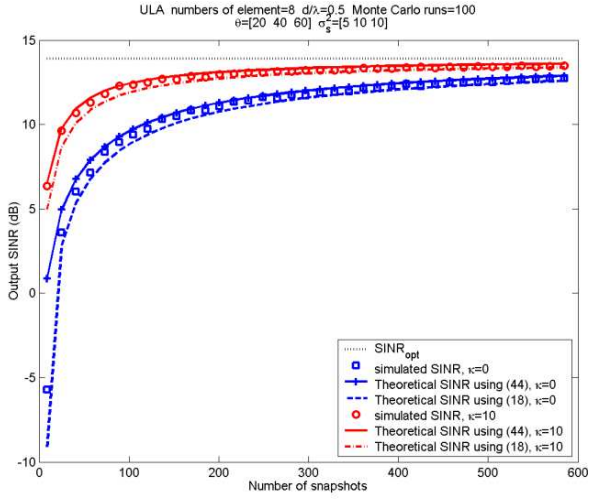

Figure 6. The output SINR versus number of data snapshots for $q = 3$.

to 0 and 10, the output SINRs and theoretical terms P_{id}, P_{nd}, and $P_{ic} + P_{nc}$ with varying desired signal power and number of snapshots are presented in Figures 4–7, respectively. In Figure 4, the theoretical results computed by (44) are almost the same as the simulated ones for $\kappa = 10$ in contrast to (18), especially for $\sigma_{s1}^2 \geq 8\,\text{dB}$. However, using (44) causes more errors than (18) for $\kappa = 0$. These errors are due to the approximations of $\hat{\mathbf{w}} \approx \mathbf{w}_o + \hat{\mathbf{w}}_c$ in (22) and $|d_{ij}|^2 \ll 1$ in derivation. The reason why the MVDR beamformer with $\kappa = 10$ is superior to the same beamformer without diagonal loading can be seen from Figure 5. The curves of P_{id} or P_{nd} for $\kappa = 0$ and $\kappa = 10$ are almost undistinguishable. Nonetheless, setting $\kappa = 10$ eliminates $P_{ic} + P_{nc}$ efficiently for large σ_{s1}^2 and therefore, improves the output SINR as we discussed in Section 4.2. In Figure 6, the proposed formula of (44) predicts the simulated output SINR for $\kappa = 10$ and $m < 150$ well, but the results computed by (18) are more accurate for $\kappa = 0$ and $m < 60$. Likewise, the reason of the performance improvement in the presence of diagonal loading can be interpreted with Figure 7. Again, the suppression of $P_{ic} + P_{nc}$ with a nonzero loading factor leads to higher output SINRs since $P_{id} + P_{nd}$ for $\kappa = 0$ and $\kappa = 10$ are almost the same.

Next, we consider the more general scenario of $3 \leq q < p$ and confirm the extension in Section 4.3. Figure 8 gives a comparison of the $P_{id}+P_{nd}$ in (33) and (62) according to different q's, and Figure 9 shows

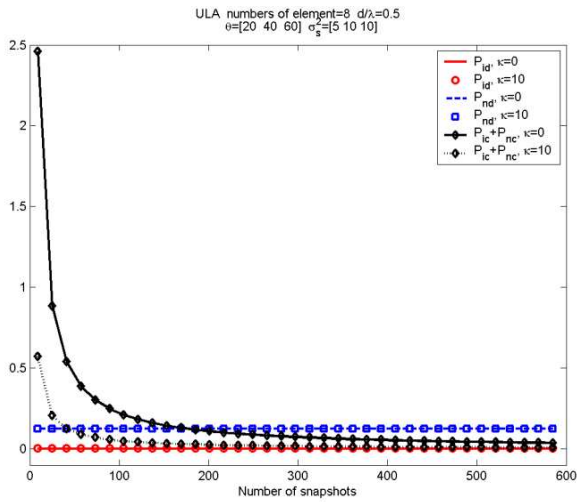

Figure 7. The theoretical terms versus number of data snapshots for $q = 3$.

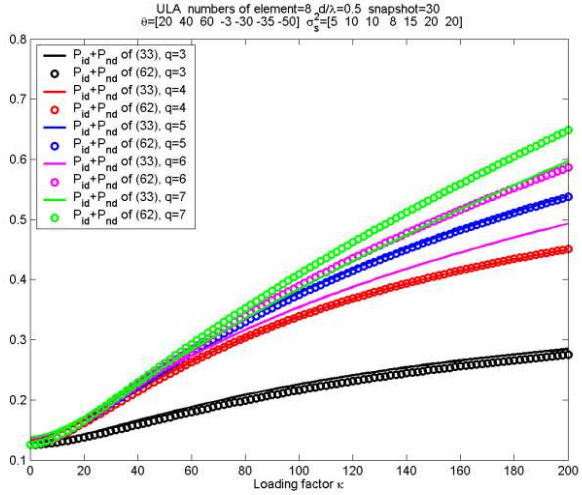

Figure 8. The $P_{id} + P_{nd}$ versus loading factor with different q's. –: using the $P_{id} + P_{nd}$ of (33). ∘: using the $P_{id} + P_{nd}$ of (62).

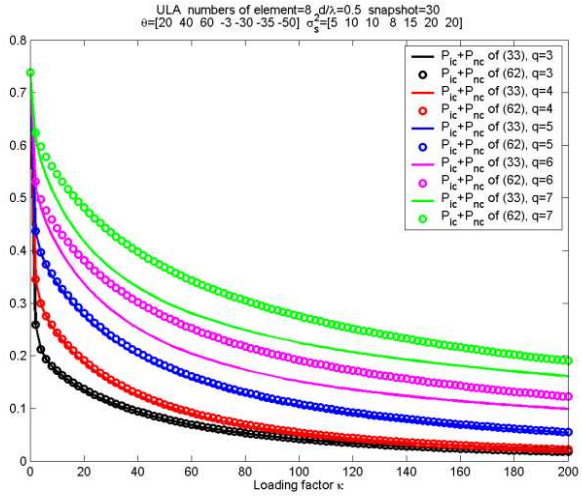

Figure 9. The $P_{ic} + P_{nc}$ versus loading factor with different q's. –: using the $P_{ic} + P_{nc}$ of (33). ∘: using the $P_{ic} + P_{nc}$ of (62).

the $P_{ic} + P_{nc}$. It is observed that the curves of the theoretical terms in (33) and (62) are close for $3 \leq q \leq 5$ but different for $6 \leq q \leq 7$. The errors for $6 \leq q \leq 7$ are attributed to the smaller angular separation between θ_5 and θ_6. The corresponding $|d_{56}|^2$ is about 0.75, which

breaks the assumption $2|d_{ij}|^2 \ll 1$ in deriving (62) and therefore, leads to more significant errors. However, the consistency between (33) and (62) for $3 \leq q \leq 5$ in this example confirms the validity of the extension from $q = 3$ to $q > 3$. Moreover, it is seen from Figures 8–9 that $P_{id}+P_{nd}$ is in general an increasing function and $P_{ic} + P_{nc}$ is a decreasing one as we analyzed the case of $q = 3$ in Sections 4.1–4.2. The accuracy

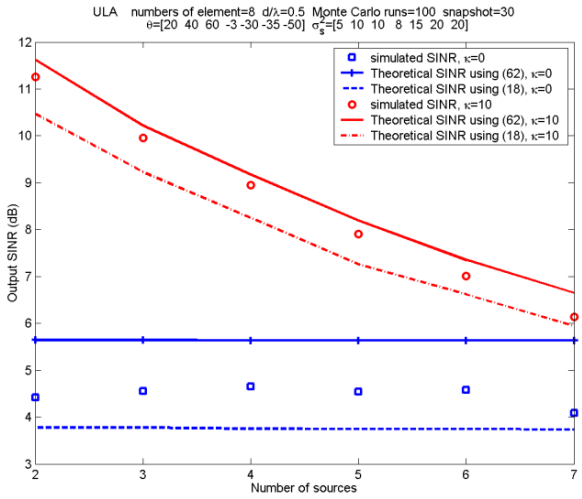

Figure 10. The output SINR versus number of sources.

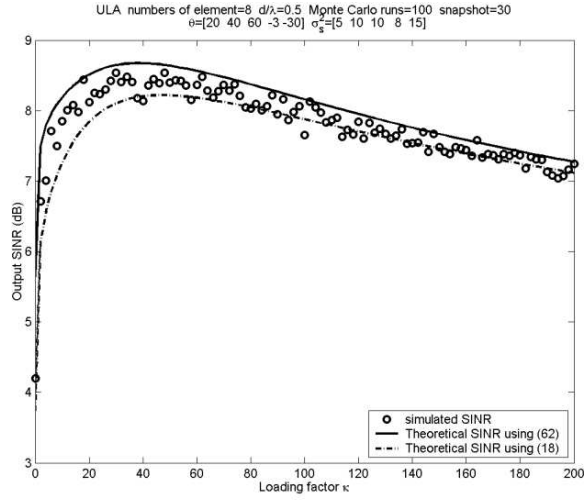

Figure 11. The output SINR versus loading factor for $q = 5$.

of (62) for $2 \leq q < p$ is examined in Figure 10, where the output SINR versus number of sources is plotted. The curve of (62) predicts the output SINR well in the presence of loading factor. It is noted that the performance of the MVDR beamformer with diagonal loading could be degraded with the growth of q. On the other hand, the output

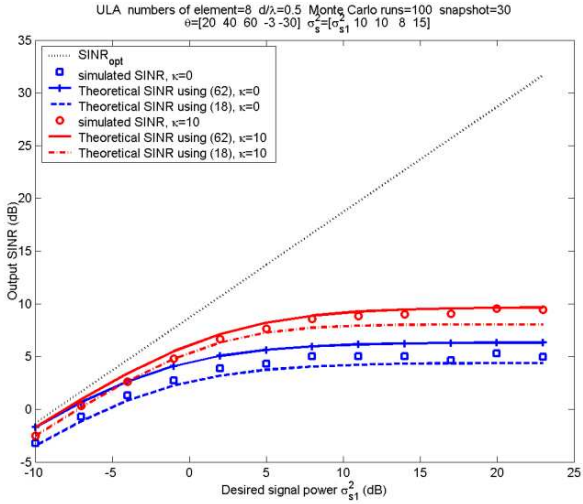

Figure 12. The output SINR versus desired signal power for $q = 5$.

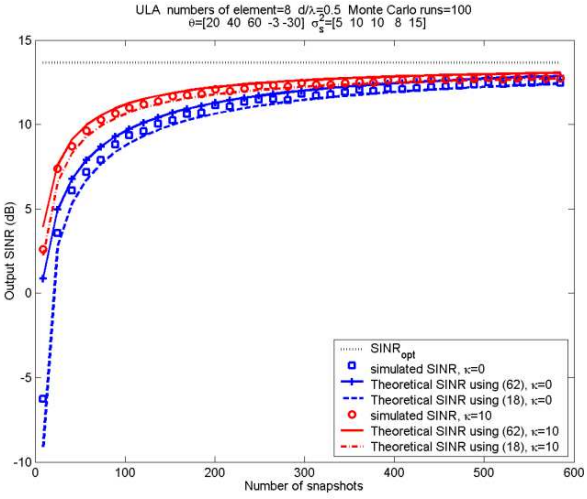

Figure 13. The output SINR versus number of data snapshots for $q = 5$.

SINR of the conventional MVDR beamformer is almost invariant to the number of interferers. Figures 11–13 are corresponding to Figures 2, 4, and 6, respectively, but with q equal to 5. The effects of the diagonal loading factor on the array performance in Figures 11–13 are similar to Figures 2–7. Again, the validity of the extension in Section 4.3 and the accuracy of the proposed formula (62) for $q = 5$ are confirmed.

6. CONCLUSION

In this paper, approximated closed-form formulas for the output SINR of MVDR array beamformers with diagonal loading under finite data samples are derived. The conventional MVDR beamformer without diagonal loading and the diagonal-loaded MVDR beamformer without finite sample effect are special cases of our research work. The provided output SINR expressions are more useful and comprehensive than the existing formula in the literature. According to the theoretical analysis, the effects of the positive loading factor on the performance of MVDR beamformers can be clearly explained. Moreover, the presented closed-form could be applied to a general situation with one desired signal and multiple interferers. Simulation results have been presented for confirming the validity of the theoretical results and making comparison with the existing results.

APPENDIX A.

The functions mentioned in Section 3 are provided in this appendix. The variables $\mathbf{Z}_a$, z_b, z_c, z_d, z_e, z_f, and $\mathbf{z}_g$ are defined as $\mathbf{Z}_a \equiv \mathbf{a}_2\mathbf{a}_2^H + \mathbf{a}_3\mathbf{a}_3^H - d_{23}^*\mathbf{a}_3\mathbf{a}_2^H - d_{23}\mathbf{a}_2\mathbf{a}_3^H$, $z_b \equiv 1 - |d_{23}|^2$, $z_c \equiv 1 - |d_{23}|^2 - |d_{12}|^2 - |d_{13}|^2 + z_d$, $z_d \equiv 2\mathrm{Re}(d_{12}d_{13}^*d_{23})$, $z_e \equiv d_{12} - d_{13}d_{23}^*$, $z_f \equiv d_{13} - d_{12}d_{23}$, and $\mathbf{z}_g \equiv z_b\mathbf{a}_1 - z_e^*\mathbf{a}_2 - z_f^*\mathbf{a}_3$, respectively. $\mathrm{Re}\{\cdot\}$ denotes the real part of a complex number.

$$\mathbf{a}_1^H\mathbf{Q}_D^{-1}\mathbf{a}_1 = \frac{\begin{array}{c} p\tilde{\sigma}_n^{-2}\left[\tilde{\sigma}_n^4 + p\sigma_{s2}^2\tilde{\sigma}_n^2\left(1-|d_{12}|^2\right)\right. \\ \left. +p\sigma_{s3}^2\tilde{\sigma}_n^2\left(1-|d_{13}|^2\right) + p^2\sigma_{s2}^2\sigma_{s3}^2 z_c\right] \end{array}}{\tilde{\sigma}_n^4 + p\sigma_{s2}^2\tilde{\sigma}_n^2 + p\sigma_{s3}^2\tilde{\sigma}_n^2 + p^2\sigma_{s2}^2\sigma_{s3}^2 z_b}, \tag{A1}$$

$$\mathbf{a}_1^H\mathbf{Q}_D^{-1}\mathbf{a}_2 = \frac{p\tilde{\sigma}_n^{-2}\left(\tilde{\sigma}_n^4 d_{12} + p\sigma_{s3}^2\tilde{\sigma}_n^2 z_e\right)}{\tilde{\sigma}_n^4 + p\sigma_{s2}^2\tilde{\sigma}_n^2 + p\sigma_{s3}^2\tilde{\sigma}_n^2 + p^2\sigma_{s2}^2\sigma_{s3}^2 z_b}, \tag{A2}$$

$$\mathbf{a}_1^H\mathbf{Q}_D^{-1}\mathbf{a}_3 = \frac{p\tilde{\sigma}_n^{-2}\left(\tilde{\sigma}_n^4 d_{13} + p\sigma_{s2}^2\tilde{\sigma}_n^2 z_f\right)}{\tilde{\sigma}_n^4 + p\sigma_{s2}^2\tilde{\sigma}_n^2 + p\sigma_{s3}^2\tilde{\sigma}_n^2 + p^2\sigma_{s2}^2\sigma_{s3}^2 z_b}, \tag{A3}$$

$$\left\|\mathbf{Q}_D^{-1}\mathbf{a}_1\right\|^2 = \frac{p\tilde{\sigma}_n^{-4}\begin{bmatrix}\tilde{\sigma}_n^8 + p\sigma_{s2}^2\tilde{\sigma}_n^4\left(p\sigma_{s2}^2+2\tilde{\sigma}_n^2\right)\left(1-\left|d_{12}\right|^2\right)\\ +p\sigma_{s3}^2\tilde{\sigma}_n^4\left(p\sigma_{s3}^2+2\tilde{\sigma}_n^2\right)\left(1-\left|d_{13}\right|^2\right)\\ +2p^2\sigma_{s2}^2\sigma_{s3}^2\tilde{\sigma}_n^4\Big(2-\left|d_{23}\right|^2-2\left|d_{12}\right|^2\\ -2\left|d_{13}\right|^2+1.5z_d\Big)\\ +p^3\sigma_{s2}^2\sigma_{s3}^2\left(2\sigma_{s2}^2\tilde{\sigma}_n^2+2\sigma_{s3}^2\tilde{\sigma}_n^2+p\sigma_{s2}^2\sigma_{s3}^2z_b\right)z_c\end{bmatrix}}{\left(\tilde{\sigma}_n^4+p\sigma_{s2}^2\tilde{\sigma}_n^2+p\sigma_{s3}^2\tilde{\sigma}_n^2+p^2\sigma_{s2}^2\sigma_{s3}^2z_b\right)^2}, \quad \text{(A4)}$$

$$\mathbf{Q}_D^{-1}\mathbf{Q} = \frac{\left\{\begin{array}{l}\tilde{\sigma}_n^4\mathbf{Q}+\sigma_n^2\tilde{\sigma}_n^2\left[\left(p\sigma_{s2}^2+p\sigma_{s3}^2+\sigma_n^2\right)\mathbf{I}-\mathbf{Q}\right]\\ +p\sigma_{s2}^2\sigma_{s3}^2\tilde{\sigma}_n^2\mathbf{Z}_a+p\sigma_{s2}^2\sigma_{s3}^2\sigma_n^2\left(pz_b\mathbf{I}-\mathbf{Z}_a\right)\end{array}\right\}}{\tilde{\sigma}_n^2\left(\tilde{\sigma}_n^4+p\sigma_{s2}^2\tilde{\sigma}_n^2+p\sigma_{s3}^2\tilde{\sigma}_n^2+p^2\sigma_{s2}^2\sigma_{s3}^2z_b\right)}, \quad \text{(A5)}$$

$$\mathbf{Q}_D^{-1}\mathbf{Q}\mathbf{Q}_D^{-1}\mathbf{Q} = \frac{\left\{\begin{array}{l}\tilde{\sigma}_n^8\mathbf{Q}\mathbf{Q}+2\sigma_n^2\tilde{\sigma}_n^6\left[\left(p\sigma_{s2}^2+p\sigma_{s3}^2+\sigma_n^2\right)\mathbf{Q}-\mathbf{Q}\mathbf{Q}\right]\\ +\sigma_n^4\tilde{\sigma}_n^4\left[\left(p\sigma_{s2}^2+p\sigma_{s3}^2+\sigma_n^2\right)\mathbf{I}-\mathbf{Q}\right]^2\\ +p\sigma_{s2}^2\sigma_{s3}^2\tilde{\sigma}_n^6\left(\mathbf{Q}\mathbf{Z}_a+\mathbf{Z}_a\mathbf{Q}\right)\\ +p\sigma_{s2}^2\sigma_{s3}^2\sigma_n^2\tilde{\sigma}_n^4\Big[2\left(p\sigma_{s2}^2+p\sigma_{s3}^2+\sigma_n^2\right)\mathbf{Z}_a\\ +\mathbf{Q}\left(pz_b\mathbf{I}-2\mathbf{Z}_a\right)+\left(pz_b\mathbf{I}-2\mathbf{Z}_a\right)\mathbf{Q}\Big]\\ +p\sigma_{s2}^2\sigma_{s3}^2\sigma_n^4\tilde{\sigma}_n^2\Big[2\left(p\sigma_{s2}^2+p\sigma_{s3}^2+\sigma_n^2\right)\left(pz_b\mathbf{I}-\mathbf{Z}_a\right)\\ -\mathbf{Q}\left(pz_b\mathbf{I}-\mathbf{Z}_a\right)-\left(pz_b\mathbf{I}-\mathbf{Z}_a\right)\mathbf{Q}\Big]\\ +p^3\sigma_{s2}^4\sigma_{s3}^4\tilde{\sigma}_n^4z_b\mathbf{Z}_a+p^3\sigma_{s2}^4\sigma_{s3}^4\sigma_n^4z_b\left(pz_b\mathbf{I}-\mathbf{Z}_a\right)\end{array}\right\}}{\tilde{\sigma}_n^4\left(\tilde{\sigma}_n^4+p\sigma_{s2}^2\tilde{\sigma}_n^2+p\sigma_{s3}^2\tilde{\sigma}_n^2+p^2\sigma_{s2}^2\sigma_{s3}^2z_b\right)^2}, \quad \text{(A6)}$$

$$\Omega_1 \approx \frac{\left\{\begin{array}{l}p\sigma_n^4\tilde{\sigma}_n^8+2p\sigma_{s2}^2\sigma_n^2\tilde{\sigma}_n^6\left[\tilde{\sigma}_n^2+(p-1)\sigma_n^2\right]\\ +2p\sigma_{s3}^2\sigma_n^2\tilde{\sigma}_n^6\left[\tilde{\sigma}_n^2+(p-1)\sigma_n^2\right]\\ +p^2\sigma_{s2}^4\tilde{\sigma}_n^4\left[\tilde{\sigma}_n^4+(p-1)\sigma_n^4\right]+p^2\sigma_{s3}^4\tilde{\sigma}_n^4\left[\tilde{\sigma}_n^4+(p-1)\sigma_n^4\right]\\ +2p^2\sigma_{s2}^2\sigma_{s3}^2\tilde{\sigma}_n^4\left[\left|d_{23}\right|^2\tilde{\sigma}_n^4+4\sigma_n^2\tilde{\sigma}_n^2+(2p-4)\sigma_n^4\right]\\ +p^4\sigma_{s2}^4\sigma_{s3}^4\left[2\tilde{\sigma}_n^4+(p-2)\sigma_n^4\right]\\ +2p^3\sigma_{s2}^4\sigma_{s3}^2\tilde{\sigma}_n^2\left[\tilde{\sigma}_n^4+\sigma_n^2\tilde{\sigma}_n^2+(p-2)\sigma_n^4\right]\\ +2p^3\sigma_{s2}^2\sigma_{s3}^4\tilde{\sigma}_n^2\left[\tilde{\sigma}_n^4+\sigma_n^2\tilde{\sigma}_n^2+(p-2)\sigma_n^4\right]\end{array}\right\}}{\tilde{\sigma}_n^4\left(p\sigma_{s2}^2+\tilde{\sigma}_n^2\right)^2\left(p\sigma_{s3}^2+\tilde{\sigma}_n^2\right)^2}, \quad \text{(A7)}$$

$$\Omega_2 \approx \frac{\left\{\begin{array}{l}\sigma_n^4\tilde{\sigma}_n^{12}+p\sigma_{s2}^2\sigma_n^2\tilde{\sigma}_n^{10}\left(2\left|d_{12}\right|^2\tilde{\sigma}_n^2+3\sigma_n^2\right)\\ +p\sigma_{s3}^2\sigma_n^2\tilde{\sigma}_n^{10}\left(2\left|d_{13}\right|^2\tilde{\sigma}_n^2+3\sigma_n^2\right)\\ +p^2\sigma_{s2}^4\tilde{\sigma}_n^8\left(\left|d_{12}\right|^2\tilde{\sigma}_n^4+3\sigma_n^4\right)\\ +p^2\sigma_{s3}^4\tilde{\sigma}_n^8\left(\left|d_{13}\right|^2\tilde{\sigma}_n^4+3\sigma_n^4\right)\\ +p^2\sigma_{s2}^2\sigma_{s3}^2\tilde{\sigma}_n^8\left[z_d\tilde{\sigma}_n^4+9\sigma_n^4+6\left(\left|d_{12}\right|^2+\left|d_{13}\right|^2-z_d\right)\sigma_n^2\tilde{\sigma}_n^2\right]\\ +p^3\sigma_{s2}^4\sigma_{s3}^2\tilde{\sigma}_n^6\left[3\left|d_{12}\right|^2\tilde{\sigma}_n^4+9\sigma_n^4+6\left(\left|d_{13}\right|^2-z_d\right)\sigma_n^2\tilde{\sigma}_n^2\right]\\ +p^3\sigma_{s2}^2\sigma_{s3}^4\tilde{\sigma}_n^6\left[3\left|d_{13}\right|^2\tilde{\sigma}_n^4+9\sigma_n^4+6\left(\left|d_{12}\right|^2-z_d\right)\sigma_n^2\tilde{\sigma}_n^2\right]\\ +p^3\sigma_{s2}^6\sigma_n^4\tilde{\sigma}_n^6+p^3\sigma_{s3}^6\sigma_n^4\tilde{\sigma}_n^6\\ +p^4\sigma_{s2}^4\sigma_{s3}^4\tilde{\sigma}_n^4\left[3\left(\left|d_{12}\right|^2+\left|d_{13}\right|^2-z_d\right)\tilde{\sigma}_n^4+9\sigma_n^4\right.\\ \left.+2\left(2\left|d_{12}\right|^2\left|d_{23}\right|^2+2\left|d_{13}\right|^2\left|d_{23}\right|^2-z_d\right)\sigma_n^2\tilde{\sigma}_n^2\right]\\ +p^4\sigma_{s2}^2\sigma_{s3}^6\tilde{\sigma}_n^4\left[2\left(\left|d_{12}\right|^2-z_d\right)\sigma_n^2\tilde{\sigma}_n^2+3\sigma_n^4\right]\\ +p^4\sigma_{s2}^6\sigma_{s3}^2\tilde{\sigma}_n^4\left[2\left(\left|d_{13}\right|^2-z_d\right)\sigma_n^2\tilde{\sigma}_n^2+3\sigma_n^4\right]\\ +p^5\sigma_{s2}^4\sigma_{s3}^6\tilde{\sigma}_n^2\left[\left(\left|d_{12}\right|^2-z_d\right)\tilde{\sigma}_n^4+3\sigma_n^4\right]\\ +p^5\sigma_{s2}^6\sigma_{s3}^4\tilde{\sigma}_n^2\left[\left(\left|d_{13}\right|^2-z_d\right)\tilde{\sigma}_n^4+3\sigma_n^4\right]+p^6\sigma_{s2}^6\sigma_{s3}^6\sigma_n^4\end{array}\right\}}{\tilde{\sigma}_n^4\left(p\sigma_{s2}^2+\tilde{\sigma}_n^2\right)^3\left(p\sigma_{s3}^2+\tilde{\sigma}_n^2\right)^3}, \quad \text{(A8)}$$

$$\Omega_3 \approx \frac{\left\{\begin{array}{l}\sigma_n^2\tilde{\sigma}_n^8+p\sigma_{s2}^2\tilde{\sigma}_n^6\left(\tilde{\sigma}_n^2\left|d_{12}\right|^2+2\sigma_n^2\right)\\ +p\sigma_{s3}^2\tilde{\sigma}_n^6\left(\tilde{\sigma}_n^2\left|d_{13}\right|^2+2\sigma_n^2\right)\\ +2p^2\sigma_{s2}^2\sigma_{s3}^2\tilde{\sigma}_n^4\left[\tilde{\sigma}_n^2\left(\left|d_{12}\right|^2+\left|d_{13}\right|^2-z_d\right)+2\sigma_n^2\right]\\ +p^2\sigma_{s2}^4\sigma_n^2\tilde{\sigma}_n^4+p^2\sigma_{s3}^4\sigma_n^2\tilde{\sigma}_n^4+p^4\sigma_{s2}^4\sigma_{s3}^4\sigma_n^2\\ +p^3\sigma_{s2}^4\sigma_{s3}^2\tilde{\sigma}_n^2\left[\tilde{\sigma}_n^2\left(\left|d_{13}\right|^2-z_d\right)+2\sigma_n^2\right]\\ +p^3\sigma_{s2}^2\sigma_{s3}^4\tilde{\sigma}_n^2\left[\tilde{\sigma}_n^2\left(\left|d_{12}\right|^2-z_d\right)+2\sigma_n^2\right]\end{array}\right\}}{\tilde{\sigma}_n^2\left(p\sigma_{s2}^2+\tilde{\sigma}_n^2\right)^2\left(p\sigma_{s3}^2+\tilde{\sigma}_n^2\right)^2}. \quad \text{(A9)}$$

APPENDIX B.

In this appendix, we explain the details about the approximation from (42) to (43). Reorganizing the terms in the square bracket of (42),

$P_{ic} + P_{nc}$ can be expressed by

$$P_{ic} + P_{nc} \approx \frac{\sigma_{s1}^2}{m} \left(\Psi_1 + \Psi_2 + \Psi_3 + \Psi_4 \right), \tag{B1}$$

where

$$\Psi_1 \equiv \sum_{r=2}^{3} \frac{\kappa p \sigma_{sr}^2 \sigma_n^2}{\left(\sigma_n^2+\kappa\right)^2 \left(p\sigma_{sr}^2+\sigma_n^2+\kappa\right)}, \quad \Psi_2 \equiv \sum_{r=2}^{3} \frac{\kappa p \sigma_{sr}^2 \left(p\sigma_{sr}^2+\sigma_n^2\right)}{\left(\sigma_n^2+\kappa\right) \left(p\sigma_{sr}^2+\sigma_n^2+\kappa\right)^2},$$

$$\Psi_3 \equiv \frac{2p^2\sigma_{s2}^2\sigma_{s3}^2 \left(\sigma_n^2+\kappa\right)^2 |d_{23}|^2}{\left(p\sigma_{s2}^2+\sigma_n^2+\kappa\right)^2 \left(p\sigma_{s3}^2+\sigma_n^2+\kappa\right)^2}, \text{ and } \Psi_4 \equiv \frac{\sigma_n^4}{\left(\sigma_n^2+\kappa\right)^2}(p-1) \tag{B2}$$

are defined for the ease of discussion. First, we compare the magnitudes of Ψ_2 and Ψ_3. According to the inequality of arithmetic and geometric means, the lower bound of Ψ_2 is given by

$$\begin{aligned} \Psi_2 \geq\ & \frac{2p\sigma_{s2}\sigma_{s3}\sqrt{\left(p\sigma_{s2}^2+\sigma_n^2\right)\left(p\sigma_{s3}^2+\sigma_n^2\right)}\left(p\sigma_{s2}^2+\sigma_n^2+\kappa\right)\left(p\sigma_{s3}^2+\sigma_n^2+\kappa\right)}{\left(p\sigma_{s2}^2+\sigma_n^2+\kappa\right)^2 \left(p\sigma_{s3}^2+\sigma_n^2+\kappa\right)^2} \\ & \times \frac{\kappa}{\sigma_n^2+\kappa}. \end{aligned} \tag{B3}$$

It can be shown that $\kappa/(\sigma_n^2+\kappa)$ is an increasing function of κ for $\kappa \geq 0$ by examining its first derivative. Comparing (B3) and Ψ_3 in (B2), we notice that Ψ_3 can be neglected when $\kappa \geq \sigma_n^2$ and $2|d_{23}|^2 \ll 1$ hold. Besides, the condition $2|d_{23}|^2 \ll 1$ can be relaxed with the growth of interference powers. For instance, if $p\sigma_{s2}^2 \geq (\sigma_n^2+\kappa)$ and $p\sigma_{s3}^2 \geq (\sigma_n^2+\kappa)$, the condition required for approximating Ψ_3 would be relaxed to $|d_{23}|^2 \ll 2$. As to the case of $\kappa \leq \sigma_n^2$, we consider $\Psi_3 + \Psi_4$ given by

$$\Psi_3 + \Psi_4 = \frac{\begin{array}{l} 2p^2\sigma_{s2}^2\sigma_{s3}^2 \left(\sigma_n^2+\kappa\right)^4 |d_{23}|^2 \\ +(p-1)\left(p\sigma_{s2}^2+\sigma_n^2+\kappa\right)^2 \left(p\sigma_{s3}^2+\sigma_n^2+\kappa\right)^2 \sigma_n^4 \end{array}}{\left(p\sigma_{s2}^2+\sigma_n^2+\kappa\right)^2 \left(p\sigma_{s3}^2+\sigma_n^2+\kappa\right)^2 \left(\sigma_n^2+\kappa\right)^2}. \tag{B4}$$

In the numerator of (B4), it is easy to show that $(\sigma_n^2+\kappa)^4$ is an increasing function of κ for $\kappa \geq 0$. Therefore, the maximum of $2p^2\sigma_{s2}^2\sigma_{s3}^2(\sigma_n^2+\kappa)^4|d_{23}|^2$ for $0 \leq \kappa \leq \sigma_n^2$ is $32p^2\sigma_{s2}^2\sigma_{s3}^2\sigma_n^4 \times \sigma_n^4|d_{23}|^2$. On the other hand, applying the inequality of arithmetic and geometric means to the second term of the numerator yields

$$\begin{aligned} & (p-1)\left(p\sigma_{s2}^2+\sigma_n^2+\kappa\right)^2 \left(p\sigma_{s3}^2+\sigma_n^2+\kappa\right)^2 \sigma_n^4 \\ \geq\ & (p-1)\, 16p^2\sigma_{s2}^2\sigma_{s3}^2\sigma_n^4 \times \left(\sigma_n^2+\kappa\right)^2. \end{aligned} \tag{B5}$$

From the assumptions of $q = 3 < p$ and $|d_{23}|^2 \ll 1$, the comparison of $\Psi_3 + \Psi_4$ indicates that $\Psi_3 \ll \Psi_4$ for $0 \le \kappa \le \sigma_n^2$. Based on the observation and discussion above, we conclude Ψ_3 is relative marginal in $P_{ic} + P_{nc}$ and can be neglected by assuming $2|d_{23}|^2 \ll 1$.

APPENDIX C.

In this appendix, we apply the well-known mathematical induction [32, 33] to prove the output SINR in (61) is a reasonable approximated result of (35) after expanding $\mathbf{Q}_D^{-1}$. First, substituting $q = 2$ into (61) yields the result of (59), which is shown to be true in Section 4.3. Next, we suppose that the P_{id} and P_{nd} in (35) can be derived and simplified to those in (61) for $q = v$. Then, we have

$$P_{id(v)} = \sum_{r=2}^{v} \sigma_{sr}^2 \left| \frac{\mathbf{a}_1^H \mathbf{Q}_{D(v)}^{-1} \mathbf{a}_r}{\mathbf{a}_1^H \mathbf{Q}_{D(v)}^{-1} \mathbf{a}_1} \right|^2 \approx \sum_{r=2}^{v} \frac{\sigma_{sr}^2 \left(\sigma_n^2 + \kappa\right)^2 |d_{1r}|^2}{\left(\sigma_n^2 + \kappa + p\sigma_{sr}^2\right)^2}, \quad \text{(C1)}$$

$$P_{nd(v)} = \sigma_n^2 \frac{\left\| \mathbf{Q}_{D(v)}^{-1} \mathbf{a}_1 \right\|^2}{\left(\mathbf{a}_1^H \mathbf{Q}_{D(v)}^{-1} \mathbf{a}_1 \right)^2} \approx \frac{\sigma_n^2}{p}, \quad \text{(C2)}$$

where the subscript (v) denotes the particular case of $q = v$. Based on (C1) and (C2), we then show that the output SINR of (61) can be derived from (35) under $q = v + 1$.

Since the analysis in Section 3.1 is suitable for a general q, we apply (27) to obtain the P_{id} for $q = v + 1$ as follows:

$$\begin{aligned} P_{id(v+1)} &= \sum_{r=2}^{v+1} \sigma_{sr}^2 \left| \frac{\mathbf{a}_1^H \mathbf{Q}_{D(v+1)}^{-1} \mathbf{a}_r}{\mathbf{a}_1^H \mathbf{Q}_{D(v+1)}^{-1} \mathbf{a}_1} \right|^2 \\ &= \sum_{r=2}^{v} \sigma_{sr}^2 \left| \frac{\mathbf{a}_1^H \mathbf{Q}_{D(v+1)}^{-1} \mathbf{a}_r}{\mathbf{a}_1^H \mathbf{Q}_{D(v+1)}^{-1} \mathbf{a}_1} \right|^2 + \sigma_{s(v+1)}^2 \left| \frac{\mathbf{a}_1^H \mathbf{Q}_{D(v+1)}^{-1} \mathbf{a}_{v+1}}{\mathbf{a}_1^H \mathbf{Q}_{D(v+1)}^{-1} \mathbf{a}_1} \right|^2. \end{aligned} \quad \text{(C3)}$$

Applying the matrix inversion lemma to $\mathbf{Q}_{D(v+1)}^{-1}$, we have

$$\mathbf{Q}_{D(v+1)}^{-1} = \mathbf{Q}_{D(v)}^{-1} \left(\mathbf{I} - \frac{\mathbf{a}_{v+1} \mathbf{a}_{v+1}^H \mathbf{Q}_{D(v)}^{-1}}{\sigma_{s(v+1)}^{-2} + \mathbf{a}_{v+1}^H \mathbf{Q}_{D(v)}^{-1} \mathbf{a}_{v+1}} \right). \quad \text{(C4)}$$

Pre-multiplying $\mathbf{a}_1^H$ and post-multiplying $\mathbf{a}_1$ and $\mathbf{a}_r$, r=2, 3, ..., v, to $\mathbf{Q}_{D(v+1)}^{-1}$, we obtain

$$\mathbf{a}_1^H \mathbf{Q}_{D(v+1)}^{-1} \mathbf{a}_1 = \mathbf{a}_1^H \mathbf{Q}_{D(v)}^{-1} \mathbf{a}_1 - \frac{\mathbf{a}_1^H \mathbf{Q}_{D(v)}^{-1} \mathbf{a}_{v+1} \mathbf{a}_{v+1}^H \mathbf{Q}_{D(v)}^{-1} \mathbf{a}_1}{\sigma_{s(v+1)}^{-2} + \mathbf{a}_{v+1}^H \mathbf{Q}_{D(v)}^{-1} \mathbf{a}_{v+1}} \quad \text{(C5)}$$

$$\text{and} \quad \mathbf{a}_1^H \mathbf{Q}_{D(v+1)}^{-1} \mathbf{a}_r = \mathbf{a}_1^H \mathbf{Q}_{D(v)}^{-1} \mathbf{a}_r - \frac{\mathbf{a}_1^H \mathbf{Q}_{D(v)}^{-1} \mathbf{a}_{v+1} \mathbf{a}_{v+1}^H \mathbf{Q}_{D(v)}^{-1} \mathbf{a}_r}{\sigma_{s(v+1)}^{-2} + \mathbf{a}_{v+1}^H \mathbf{Q}_{D(v)}^{-1} \mathbf{a}_{v+1}}. \quad \text{(C6)}$$

Now, consider the diagonal-loaded weight vector $\mathbf{w}_1 = \mathbf{Q}_{D(v)}^{-1} \mathbf{a}_1$ without normalized scalar. Since $\mathbf{Q}_{D(v)}$ contains the 2nd to vth signal sources, the directions of $\mathbf{a}_1$, $\mathbf{a}_{v+1}$, and $\mathbf{a}_r$, $r = 2, 3, \ldots, v$, are regarded as the desired signal, noise, and interference, respectively. The responses of $\mathbf{w}_1$ in the three directions are different and in general, $\mathbf{w}_1^H \mathbf{a}_1$ is much larger than $\mathbf{w}_1^H \mathbf{a}_{v+1}$ and $\mathbf{w}_1^H \mathbf{a}_r$. Therefore,

$$\begin{aligned} \mathbf{a}_1^H \mathbf{Q}_{D(v)}^{-1} \mathbf{a}_1 &\gg \mathbf{a}_1^H \mathbf{Q}_{D(v)}^{-1} \mathbf{a}_{v+1} \\ \text{and} \quad \mathbf{a}_1^H \mathbf{Q}_{D(v)}^{-1} \mathbf{a}_1 &\gg \mathbf{a}_1^H \mathbf{Q}_{D(v)}^{-1} \mathbf{a}_r. \end{aligned} \quad \text{(C7)}$$

On the other hand, if the steering vector of the desired signal becomes $\mathbf{a}_{v+1}$, the according weight vector is $\mathbf{w}_2 = \mathbf{Q}_{D(v)}^{-1} \mathbf{a}_{v+1}$. To $\mathbf{w}_2$, the directions of $\mathbf{a}_1$, $\mathbf{a}_{v+1}$, and $\mathbf{a}_r$ are identified as the noise, desired signal, and interference, respectively. Similarly, we have

$$\begin{aligned} \mathbf{a}_{v+1}^H \mathbf{Q}_{D(v)}^{-1} \mathbf{a}_{v+1} &\gg \mathbf{a}_{v+1}^H \mathbf{Q}_{D(v)}^{-1} \mathbf{a}_1 \\ \text{and} \quad \mathbf{a}_{v+1}^H \mathbf{Q}_{D(v)}^{-1} \mathbf{a}_{v+1} &\gg \mathbf{a}_{v+1}^H \mathbf{Q}_{D(v)}^{-1} \mathbf{a}_r. \end{aligned} \quad \text{(C8)}$$

Note that (C7) and (C8) hold because the 1st and $(v+1)$th sources are excluded from $\mathbf{Q}_{D(v)}$ and all the $(v+1)$ sources are assumed to be separate enough so that $|d_{ij}|^2 \ll 1$, $i \neq j$. Combining (C7) and (C8) yields

$$\mathbf{a}_1^H \mathbf{Q}_{D(v)}^{-1} \mathbf{a}_1 \approx \mathbf{a}_{v+1}^H \mathbf{Q}_{D(v)}^{-1} \mathbf{a}_{v+1} \gg \mathbf{a}_1^H \mathbf{Q}_{D(v)}^{-1} \mathbf{a}_{v+1} \approx \mathbf{a}_{v+1}^H \mathbf{Q}_{D(v)}^{-1} \mathbf{a}_1$$

and

$$\mathbf{a}_1^H \mathbf{Q}_{D(v)}^{-1} \mathbf{a}_1 \approx \mathbf{a}_{v+1}^H \mathbf{Q}_{D(v)}^{-1} \mathbf{a}_{v+1} \gg \mathbf{a}_1^H \mathbf{Q}_{D(v)}^{-1} \mathbf{a}_r \approx \mathbf{a}_{v+1}^H \mathbf{Q}_{D(v)}^{-1} \mathbf{a}_r. \quad \text{(C9)}$$

According to (C9), $\mathbf{a}_1^H \mathbf{Q}_{D(v+1)}^{-1} \mathbf{a}_1$ in (C5) and $\mathbf{a}_1^H \mathbf{Q}_{D(v+1)}^{-1} \mathbf{a}_r$ in (C6) can be approximated to

$$\mathbf{a}_1^H \mathbf{Q}_{D(v+1)}^{-1} \mathbf{a}_1 \approx \mathbf{a}_1^H \mathbf{Q}_{D(v)}^{-1} \mathbf{a}_1 \quad \text{(C10)}$$

$$\text{and} \quad \mathbf{a}_1^H \mathbf{Q}_{D(v+1)}^{-1} \mathbf{a}_r \approx \mathbf{a}_1^H \mathbf{Q}_{D(v)}^{-1} \mathbf{a}_r, \quad \text{(C11)}$$

respectively. Using (C1), (C10), and (C11), the summation term on the right-hand side of (C3) can be approximated to

$$\begin{aligned} \sum_{r=2}^{v} \sigma_{sr}^2 \left| \frac{\mathbf{a}_1^H \mathbf{Q}_{D(v+1)}^{-1} \mathbf{a}_r}{\mathbf{a}_1^H \mathbf{Q}_{D(v+1)}^{-1} \mathbf{a}_1} \right|^2 &\approx \sum_{r=2}^{v} \sigma_{sr}^2 \left| \frac{\mathbf{a}_1^H \mathbf{Q}_{D(v)}^{-1} \mathbf{a}_r}{\mathbf{a}_1^H \mathbf{Q}_{D(v)}^{-1} \mathbf{a}_1} \right|^2 \\ &\approx \sum_{r=2}^{v} \frac{\sigma_{sr}^2 \left(\sigma_n^2 + \kappa\right)^2 |d_{1r}|^2}{\left(\sigma_n^2 + \kappa + p\sigma_{sr}^2\right)^2}. \end{aligned} \quad \text{(C12)}$$

Further, applying the results of (C10) and (C11), we have

$$\mathbf{a}_1^H \mathbf{Q}_{D(v+1)}^{-1} \mathbf{a}_1 \approx \mathbf{a}_1^H \dot{\mathbf{Q}}_{D(v)}^{-1} \mathbf{a}_1 \tag{C13}$$

and

$$\mathbf{a}_1^H \mathbf{Q}_{D(v+1)}^{-1} \mathbf{a}_{v+1} \approx \mathbf{a}_1^H \dot{\mathbf{Q}}_{D(v)}^{-1} \mathbf{a}_{v+1}, \tag{C14}$$

where $\dot{\mathbf{Q}}_{D(v)}$ is obtained by removing one of the 2nd to vth sources from $\mathbf{Q}_{D(v+1)}$. Analogous to each term of (C12), the second term on the right-hand side of (C3) can be approximated to

$$\begin{aligned} \sigma_{s(v+1)}^2 \left| \frac{\mathbf{a}_1^H \mathbf{Q}_{D(v+1)}^{-1} \mathbf{a}_{v+1}}{\mathbf{a}_1^H \mathbf{Q}_{D(v+1)}^{-1} \mathbf{a}_1} \right|^2 &\approx \sigma_{s(v+1)}^2 \left| \frac{\mathbf{a}_1^H \dot{\mathbf{Q}}_{D(v)}^{-1} \mathbf{a}_{v+1}}{\mathbf{a}_1^H \dot{\mathbf{Q}}_{D(v)}^{-1} \mathbf{a}_1} \right|^2 \\ &\approx \frac{\sigma_{s(v+1)}^2 \left(\sigma_n^2 + \kappa\right)^2 \left|d_{1(v+1)}\right|^2}{\left(\sigma_n^2 + \kappa + p\sigma_{s(v+1)}^2\right)^2}. \end{aligned} \tag{C15}$$

It follows from (C12) and (C15) that the P_{id} for $q = v + 1$ is given by

$$P_{id(v+1)} = \sum_{r=2}^{v+1} \sigma_{sr}^2 \left| \frac{\mathbf{a}_1^H \mathbf{Q}_{D(v+1)}^{-1} \mathbf{a}_r}{\mathbf{a}_1^H \mathbf{Q}_{D(v+1)}^{-1} \mathbf{a}_1} \right|^2 \approx \sum_{r=2}^{v+1} \frac{\sigma_{sr}^2 \left(\sigma_n^2 + \kappa\right)^2 |d_{1r}|^2}{\left(\sigma_n^2 + \kappa + p\sigma_{sr}^2\right)^2}. \tag{C16}$$

Next, consider the P_{nd} in (30) for $q = v + 1$ as follows:

$$P_{nd(v+1)} = \sigma_n^2 \frac{\left\| \mathbf{Q}_{D(v+1)}^{-1} \mathbf{a}_1 \right\|^2}{\left(\mathbf{a}_1^H \mathbf{Q}_{D(v+1)}^{-1} \mathbf{a}_1 \right)^2}, \tag{C17}$$

where the squared norm of $\mathbf{Q}_{D(v+1)}^{-1} \mathbf{a}_1$ can be derived to

$$\begin{aligned} \left\| \mathbf{Q}_{D(v+1)}^{-1} \mathbf{a}_1 \right\|^2 = \left\| \mathbf{Q}_{D(v)}^{-1} \mathbf{a}_1 \right\|^2 + \left| \frac{\mathbf{a}_{v+1}^H \mathbf{Q}_{D(v)}^{-1} \mathbf{a}_1}{\sigma_{s(v+1)}^{-2} + \mathbf{a}_{v+1}^H \mathbf{Q}_{D(v)}^{-1} \mathbf{a}_{v+1}} \right|^2 \left\| \mathbf{Q}_{D(v)}^{-1} \mathbf{a}_{v+1} \right\|^2 \\ -2\mathrm{Re}\left(\frac{\mathbf{a}_{v+1}^H \mathbf{Q}_{D(v)}^{-1} \mathbf{a}_1}{\sigma_{s(v+1)}^{-2} + \mathbf{a}_{v+1}^H \mathbf{Q}_{D(v)}^{-1} \mathbf{a}_{v+1}} \mathbf{a}_1^H \mathbf{Q}_{D(v)}^{-1} \mathbf{Q}_{D(v)}^{-1} \mathbf{a}_{v+1} \right) \end{aligned} \tag{C18}$$

according to (C4). Again, utilizing the relationship of (C9), equation (C18) can be approximated to

$$\left\| \mathbf{Q}_{D(v+1)}^{-1} \mathbf{a}_1 \right\|^2 \approx \left\| \mathbf{Q}_{D(v)}^{-1} \mathbf{a}_1 \right\|^2. \tag{C19}$$

Substituting (C19) and (C10) into (C17) and utilizing (C2) yield

$$P_{nd(v+1)} = \sigma_n^2 \frac{\left\| \mathbf{Q}_{D(v+1)}^{-1} \mathbf{a}_1 \right\|^2}{\left(\mathbf{a}_1^H \mathbf{Q}_{D(v+1)}^{-1} \mathbf{a}_1 \right)^2} \approx \sigma_n^2 \frac{\left\| \mathbf{Q}_{D(v)}^{-1} \mathbf{a}_1 \right\|^2}{\left(\mathbf{a}_1^H \mathbf{Q}_{D(v)}^{-1} \mathbf{a}_1 \right)^2} \approx \frac{\sigma_n^2}{p}. \quad \text{(C20)}$$

From the P_{id} in (C16) and P_{nd} in (C20), we have the approximated output SINR for $q = v+1$ given by

$$\begin{aligned} \mathrm{SINR}\left(\mathbf{w}_D\right)|_{q=v+1} &= \frac{\sigma_{s1}^2}{P_{id(v+1)} + P_{nd(v+1)}} \\ &\approx \sigma_{s1}^2 \left[\sum_{r=2}^{v+1} \frac{\sigma_{sr}^2 \left(\sigma_n^2 + \kappa\right)^2 |d_{1r}|^2}{\left(\sigma_n^2 + \kappa + p\sigma_{sr}^2\right)^2} + \frac{\sigma_n^2}{p} \right]^{-1}, \quad \text{(C21)} \end{aligned}$$

which is the same as (61) with q replaced by $v+1$. Therefore, it is proved by mathematical induction that the approximated SINR($\mathbf{w}_D$) in (61) is valid for $2 \leq q < p$, which also confirms the validity of the P_{id} and P_{nd} in (61) and (62).

ACKNOWLEDGMENT

This work was supported by the National Science Council of TAIWAN under Grants NSC97-2221-E002-174-MY3 and NSC100-2221-E002-200-MY3.

REFERENCES

1. Frost, O. L., "An algorithm for linearly constrained adaptive array processing," *Proc. IEEE*, Vol. 60, No. 8, 926–935, Aug. 1972.
2. Reed, I. S., J. D. Mallett, and L. E. Brennan, "Rapid convergence rate in adaptive arrays," *IEEE Trans. Aerosp. Electron. Syst.*, Vol. 10, No. 6, 853–863, Nov. 1974.
3. Monzingo, R. A. and T. W. Miller, *Introduction to Adaptive Arrays*, Wiley, New York, 1980.
4. Chang, L. and C.-C. Yeh, "Performance of DMI and eigenspace-based beamformers," *IEEE Trans. Antennas Propag.*, Vol. 40, No. 11, 1336–1347, Nov. 1992.
5. Wax, M. and Y. Anu, "Performance analysis of the minimum variance beamformer," *IEEE Trans. Signal Process.*, Vol. 44, No. 4, 928–937, Apr. 1996.
6. Carlson, B. D., "Covariance matrix estimation errors and diagonal loading in adaptive arrays," *IEEE Trans. Aerosp. Electron. Syst.*, Vol. 24, No. 4, 397–401, Jul. 1988.

7. Ganz, M. W., R. L. Moses, and S. L. Wilson, "Convergence of the SMI and the diagonally loaded SMI algorithms with weak interference," *IEEE Trans. Antennas Propag.*, Vol. 38, No. 3, 394–399, Mar. 1990.
8. Fertig, L. B., "Statistical performance of the MVDR beamformer in the presence of diagonal loading," *Proc. First IEEE SAM Workshop*, 77–81, 2000.
9. Liu, X., C. Liu, and G. Liao, "Diagonal loading for STAP and its performance analysis," *Proc. 6th IEEE WiCOM*, 2010.
10. Dilsavor, R. L. and R. L. Moses, "Analysis of modified SMI method for adaptive array weight control," *IEEE Trans. Signal Process.*, Vol. 41, No. 2, 721–726, Feb. 1993.
11. Mestre, X. and M. A. Lagunas, "Finite sample size effect on minimum variance beamformers: Optimum diagonal loading factor for large arrays," *IEEE Trans. Signal Process.*, Vol. 54, No. 1, 69–82, Jan. 2006.
12. Chen, Y.-L. and J.-H. Lee, "Finite data performance analysis of LCMV antenna array beamformers with and without signal blocking," *Progress In Electromagnetics Research*, Vol. 130, 281–317, 2012.
13. Elnashar, A., S. M. Elnoubi, and H. A. El-Mikati, "Further study on robust adaptive beamforming with optimum diagonal loading," *IEEE Trans. Antennas Propag.*, Vol. 54, No. 12, 3647–3658, Dec. 2006.
14. Lee, J.-H. and Y.-L. Chen, "Performance analysis of antenna array beamformers with mutual coupling effects," *Progress In Electromagnetics Research B*, Vol. 33, 291–315, 2011.
15. Lorenz, R. G. and S. P. Boyd, "Robust minimum variance beamforming," *IEEE Trans. Signal Process.*, Vol. 53, No. 5, 1684–1696, May 2005.
16. Li, J., P. Stoica, and Z. Wang, "On robust Capon beamforming and diagonal loading," *IEEE Trans. Signal Process.*, Vol. 51, No. 7, 1702–1715, Jul. 2003.
17. Besson, O. and F. Vincent, "Performance analysis of beamformers using generalized loading of the covariance matrix in the presence of random steering vector errors," *IEEE Trans. Signal Process.*, Vol. 53, No. 2, 452–459, Feb. 2005.
18. Wax, M. and Y. Anu, "Performance analysis of the minimum variance beamformer in the presence of steering vector errors," *IEEE Trans. Signal Process.*, Vol. 44, No. 4, 938–947, Apr. 1996.
19. Feldman, D. D. and L. J. Griffiths, "A projection approach

for robust adaptive beamforming," *IEEE Trans. Signal Process.*, Vol. 42, No. 4, 867–876, Apr. 1994.

20. Haimovich, A. M. and Y. Bar-Ness, "An eigenanalysis interference canceler," *IEEE Trans. Signal Process.*, Vol. 39, No. 1, 76–84, Jan. 1991.
21. Pillai, S. U., *Array Signal Processing*, Springer-Verlag, New York, 1989.
22. Widrow, B., K. M. Duvall, R. P. Gooch, and W. C. Newman, "Signal cancellation phenomena in adaptive antennas: Causes and cures," *IEEE Trans. Antennas Propag.*, Vol. 30, No. 3, 469–478, May 1982.
23. Hudson, J. E., *Adaptive Array Principles*, Peter Peregrinus, London, 1981.
24. Gabriel, W. F., "Using spectral estimation techniques in adaptive processing antenna systems," *IEEE Trans. Antennas Propag.*, Vol. 34, No. 3, 291–300, Mar. 1986.
25. Cox, H., R. M. Zeskind, and M. M. Owen, "Robust adaptive beamforming," *IEEE Trans. Acoust., Speech, Signal Process.*, Vol. 35, No. 10, 1365–1376, Oct. 1987.
26. Gu, J. and P. J. Wolfe, "Robust adaptive beamforming using variable loading," *Proc. Fourth IEEE SAM Workshop*, 1–5, 2006.
27. Gu, Y. J., Z. G. Shi, K. S. Chen, and Y. Li, "Robust adaptive beamforming for steering vector uncertainties based on equivalent DOAs method," *Progress In Electromagnetics Research*, Vol. 79, 277–290, 2008.
28. Liu, W. and S. Ding, "An efficient method to determine the diagonal loading factor using the constant modulus feature," *IEEE Trans. Signal Process.*, Vol. 56, No. 12, 6102–6106, Dec. 2008.
29. Du, L., J. Li, and P. Stoica, "Fully automatic computation of diagonal loading levels for robust adaptive beamforming," *IEEE Trans. Aerosp. Electron. Syst.*, Vol. 46, No. 1, 449–458, Jan. 2010.
30. Li, Y., Y. J. Gu, Z. G. Shi, and K. S. Chen, "Robust adaptive beamforming based on particle filter with noise unknown," *Progress In Electromagnetics Research*, Vol. 90, 151–169, 2009.
31. Lee, J.-H. and C.-C. Lee, "Analysis of the performance and sensitivity of an eigenspace-based interference canceler," *IEEE Trans. Antennas Propag.*, Vol. 48, No. 5, 826–835, May 2000.
32. Trim, D., *Calculus for Engineers*, Prentice Hall, Toronto, 2008.
33. Sominskii, I. S., *The Method of Mathematical Induction*, Pergamon, London, 1961.